

## Chapter 2

# Thermal Properties of Rocks and Density of Fluids

### 2.1 Thermal Conductivity

Thermal conductivity or the thermal conductivity coefficient of a material defines its ability to transfer heat. Consider an infinite plane wall of a certain material with a thickness of one unit in length. The sides of the wall are maintained at constant temperatures and the temperature difference is equal to 1 °C.

Let us also assume that a sensor can measure the amount of heat per unit of the area of the wall per unit of time. In this case the amount of heat measured will be numerically equal to the thermal conductivity coefficient ( $\lambda$ ) of the given material. The dimension of this quantity in SI is  $\text{J m}^{-1} \text{s}^{-1} \text{K}^{-1}$  or  $\text{W m}^{-1} \text{K}^{-1}$ .

It was found experimentally that the amount of heat transferred through the wall ( $q_A$ ) is proportional to the area ( $A$ ) and to ratio of the temperature difference ( $\Delta T$ ) to the wall thickness ( $\Delta x$ ). This statement is known as Fourier's law (or equation) of thermal diffusion. In the differential form, the Fourier law for a unit of area may be expressed by the formula,

$$q = -\lambda \frac{\partial T}{\partial x}, \quad (2.2.1)$$

where  $q$  is the heat flow rate in the direction of  $x$ . The negative sign is due to the fact that heat flows in the direction of lower temperatures.

Thus, the coefficient of proportionality in Eq. (2.2.1) is the thermal conductivity (in the direction of  $x$ ) coefficient. In the hydrodynamics of flow of incompressible fluids through porous media, an analogous equation was suggested by Darcy. In the Darcy equation, the flow rate is proportional to the pressure gradient and the coefficient proportionality is the permeability and hydrodynamic viscosity ratio (mobility). Similarly, in electrical current conduction, according to Ohm's formula, the current is proportional to the voltage gradient. The coefficient of proportionality here is the specific electrical conductivity. Thus there is a correspondence between the thermal conductivity coefficient, mobility, and

**Table 2.1** Thermal conductivities<sup>a</sup> of some geological materials (Poelchau et al. 1997)

Material	$\text{Wm}^{-1} \text{K}^{-1}$	Source
Earth's crust	2.0–2.5	Mean value, Kappelmeyer and Hänel (1974)
Rocks	1.2–5.9	Sass et al. (1971)
Sandstone	2.5	Clark (1966)
Shale	1.1–2.1	Clark (1966), Blackwell and Steele (1989)
Limestone	2.5–3	Clark (1966), Robertson (1979)
Water	0.6 at 20 °C	Birch et al. (1942)
Oil	0.15 at 20 °C	Birch et al. (1942)
Ice	2.1	Gretener (1981)
Air	0.025	CRC (1974) Handbook
Methane	0.033	CRC (1974) Handbook

<sup>a</sup> Please take into account that measured conductivities and some other thermal properties of rocks observed in various regions (and even within the same regions) may vary due to influence of different physical-chemical factors

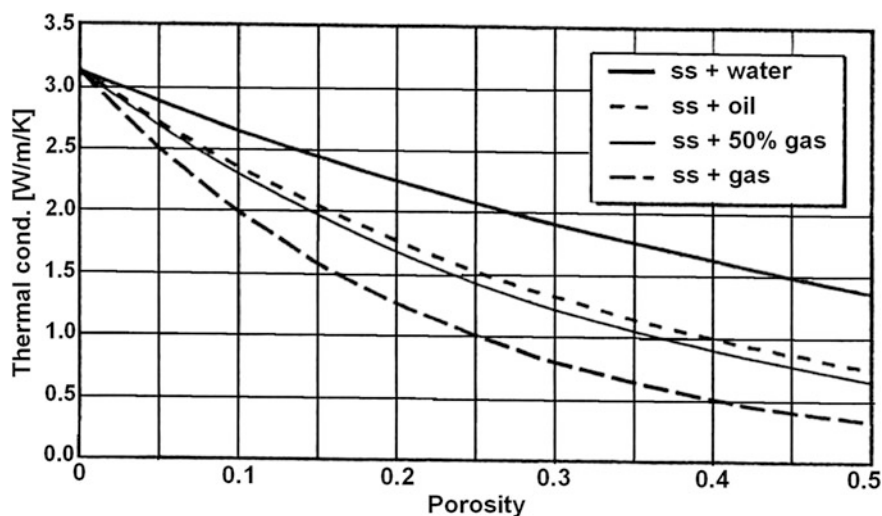


**Fig. 2.1** Thermal conductivity of sandstone as a function of porosity and pore fluid at ambient temperature and pressure (Poelchau et al. 1997)

specific electrical conductivity. The thermal conductivity of formations is dependent on temperature, pressure, porosity, composition, and properties of pore-filling fluids and gases. Values of thermal conductivity coefficients range widely for rocks and pore-filling substances (Table 2.1).

All pore-filling fluids have lower  $\lambda$  values than rocks and this causes the overall thermal conductivity to decrease with increasing porosity (Poelchau et al. 1997). Examples of the effect of porosity are presented in Fig. 2.1.

For low porosity formations, temperature has a major effect on variation of thermal conductivity (Fig. 2.2, Table 2.2).

**Fig. 2.2** Variation of the thermal conductivity of salt with temperature (Blesh et al. 1983)

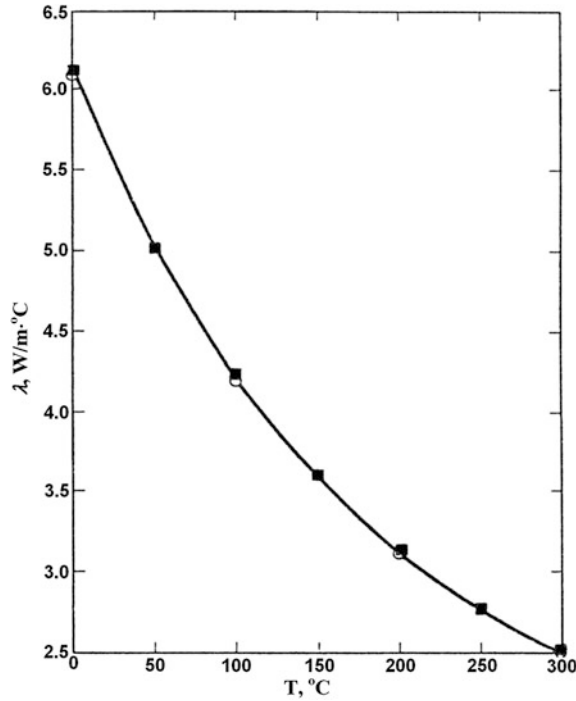


**Table 2.2** Temperature effect on thermal conductivity (values are given in  $10^{-3}$  cal/cm s °C;  $1 \times 10^{-3}$  cal/cm s °C = 41.86 m Wm<sup>-2</sup>) of sedimentary rocks (Kappelmeyer and Hänel 1974)

Formation	$\rho$ (g/cm <sup>3</sup> )	0 °C	50 °C	100 °C	200 °C	300 °C	400 °C	500 °C
Dolomite	2.83	11.9	10.30	9.30	7.95			
Limestone	2.60	7.20	6.14	5.53	4.77			
Limestone, parallel	2.60	8.24	7.55	7.04	6.54			
Limestone, perpend.	2.69	6.09	5.68	5.41				
Quartz-sandstone, parallel	2.64	13.6	11.80	10.60	9.00			
Quartz-sandstone, perpend.	2.65	13.1	11.40	10.30	8.65			
Shale			2.17	2.25	2.38	2.54	2.68	2.83
Slate, parallel	2.70	6.35	6.05	5.85	5.50	5.20	4.95	4.80
Slate, perpend.	2.76	4.83	4.40	4.23	4.08			
Calcite, parallel		27.3	22.40	19.00	15.1	12.30	10.30	
Calcite, perpend.		16.3	13.50	11.80	9.70	8.40	7.40	
Halite	2.16	14.6	12.00	10.05	7.45	5.95	4.98	

Birch and Clark (1940) suggested that the reciprocal of thermal conductivity (thermal resistivity) might be a linear function of the temperature. Blesh et al. (1983) found that the agreement between the best-fit line and experimental data for several rocks for temperatures up to 300 °C is acceptable, and does not vary by more than 3 %. Coefficients of the equation

**Table 2.3** Coefficients of the least-squares fit for thermal conductivity data (Blesh et al. 1983)

Rock	$a_0$ (m °C/W)	$a_1 \times 10^4$ (m/W)
Salt	0.1605	7.955
Granite	0.3514	3.795
Basalt	0.8684	-6.146
Shale <sub>vert</sub>	0.5297	2.215
Shale <sub>hor</sub>	0.7167	2.949

$$\lambda^{-1} = a_0 + a_1 T \quad (2.1.2)$$

are presented in Table 2.3.

As shown in Table 2.3 the thermal conductivity for shale parallel to bedding is higher than the vertical thermal conductivity. For sedimentary rocks, thermal anisotropy ratios (horizontal to vertical) up to 2.5 have been reported (Kappelmeyer and Hänel 1974; Gretener 1981; Popov et al. 1995). Kutas and Gordienko (1971) proposed the following empirical formula for estimating the thermal conductivities of sedimentary formations at temperatures of up to 300 °C,

$$\lambda_T = \lambda_{20} - (\lambda_{20} - 3.3) \left[ \exp \left( 0.725 \frac{T - 20}{T + 130} \right) - 1 \right], \quad (2.1.3)$$

where  $\lambda_{20}$  is the thermal conductivity coefficient at 20 °C in  $10^{-3}$  cal s<sup>-1</sup> cm<sup>-1</sup> °C.

This formula is accurate within 5–10 %. Only one value of  $\lambda_T$  is needed to use the latter formula. For example, let assume that the value of the thermal conductivity coefficient at  $T = 50$  °C is known. Then from the equation above the value of  $\lambda_{20}$  is calculated. The increase in thermal conductivity with pressure ( $p$ ) can be accounted for by the following equation (Kappelmeyer and Hänel 1974):

$$\lambda = \lambda_0(1 + \delta p), \quad (2.1.4)$$

where  $\lambda_0$  is the thermal conductivity coefficient at normal pressure, and  $\sigma$  is the pressure coefficient of the thermal conductivity.

Very few experiments have been conducted to estimate the values of  $\sigma$ . From experiments at pressures up to 10,000–12,000 kg cm<sup>-2</sup> the calculated values of  $\sigma$  were small: for rocksalt  $3.6 \times 10^{-5}$ ; for dry and wet limestone with a density of 2.31 g/cm<sup>3</sup>  $9.5 \times 10^{-5}$  and  $1.35 \times 10^{-5}$ ; and for dry and wet sandstone with a density of 2.64 g/cm<sup>3</sup> respectively  $2.5 \times 10^{-4}$  and  $5.7 \times 10^{-5}$  kg<sup>-1</sup> cm<sup>2</sup> (Kappelmeyer and Hänel 1974). However, at lower pressures (up to 205 kg cm<sup>-2</sup>) higher values of  $\delta$  were obtained (Hurtig and Brugger 1970, Table 2.4).

The average values of heat conductivity for certain rocks are presented in Table 2.5.

It should be noted that in Table 2.5 the values of heat conductivity listed for some rocks (for example for granites, gneisses, amphibolites, limestones) reproduced from Sharma (2002) are too high relative to other data. For example the average value of heat conductivity of granites is 3.07 W/(m K) and has a range of 2.3–3.6 W/(m K) (Sharma 2002) conflicts with the value of 2.2 W/(m K) presented

**Table 2.4** Effect of pressure on thermal conductivity of sedimentary rocks. Thermal conductivity data (Hurtig and Brugger 1970)

Sample	$\lambda$ at 0.4 kg/cm <sup>2</sup> (10 <sup>-3</sup> cal/cm s °C)	Pressure (kg/cm <sup>2</sup> )	$\delta$ (10 <sup>-3</sup> kg/cm <sup>2</sup> )
<i>Sandstone</i>			
No. 172	6.84	0.4–164	0.434
No. 224	5.51	0.4–164	0.612
No. 234	6.69	0.4–164	0.626
No. 286	7.50	0.4–164	0.931
No. 313	9.44	0.4–164	0.905
No. 343	8.51	0.4–41	3.43
<i>Limestone</i>			
No. 19	5.06	0.4–164	0.599
No. 34	4.22	0.4–164	0.185
No. 102	7.67	0.4–164	0.406
No. 260	4.33	0.4–123	0.808
No. 270	3.53	0.4–164	0.579
<i>Dolomite</i>			
No 103	7.62	0.4–123	1.71
No. 365	6.18	0.4–123	0.928

After Kappelmeyer and Hänel (1974)

in Lide (2005), which is completely out of the range reported by Sharma (2002). The value of heat conductivity for granites 2.5–2.6 W/(m K) presented by Côté and Konrad (2005) is also much smaller. At the same time, the average heat conductivity value for basalts presented by Sharma (2002) of 1.69 W/(m K) [with a range of 1.12–2.38 W/(m K)] appears too low compared even to the value of 2 W/(m K) presented in Lide (2005). However these discrepancies could have been caused by the local characteristics of the rocks and/or sampling dependence. For instance, the ranges of heat conductivity values for some rocks presented in Sharma (2002) are very wide [such as 1.35–4.86 W/(m K) for andesite; 1.82–4.73 W/(m K) for amphibolite, 1.63–6.26 W/(m K) for limestone], which can definitely render the average value sample-dependent.

Another explanation for these different and elevated values may be the varying degrees of water saturation in the samples. It is well established that samples saturated with water have much higher values of heat conductivity than dry samples (Pribnow et al. 1996; Cho et al. 2009; Shim et al. 2010). Porosity also significantly affects values of heat conductivity. Cho et al. (2009) reported that values of heat conductivity of dry granites range from 2.12 W/(m K) for rocks with high porosity to 3.12 W/(m K) for those with low porosity. The heat conductivity of rocks also depends on their mineralogical composition. For example, the heat conductivity of granites depends considerably on their quartz [ $\sim 7.69$  W/(m K)] and albite [2.14 W/(m K)] (Kim et al. 2007) content, two key components of this rock. In addition, in different localities even the same kinds of rock could have been formed under different conditions and can have significantly different heat

**Table 2.5** Average values of heat conductivity  $\lambda$  of certain rocks [in W/(m K)]

Rock	From published data <sup>a</sup>		After Sharma (2002)
	No. of samples	Average heat conductivity	Average heat conductivity
Sand	1,149	1.79	1.1–2.1
Siltstone	476	1.58	–
Argillite, clay schist	783	1.67	2.09
Clay	660	1.43	0.8–1.5
Marl	217	1.78	–
Limestone	781	2.37	3.44
Chock	21	1.63	–
Granite	383	2.68	3.07
Granodiorite	83	2.79	2.63
Porphyrite	137	1.74	–
Diorite	78	2.10	2.5
Andesites, andesite-basalt	81	1.87	2.26
Basalt	98	2.11	1.69
Diabase	67	2.50	2.2
Gabbro	116	2.47	2.57
Schist	181	2.55	–
Gneiss	88	2.41	2.7–3.1
Amphibolite	47	2.39	3.33
Gneiss-granite	35	2.04	–
Quartzite	–	5.00	5.03
Anhydrite	–	–	5.43
Harzburgite	106	2.69	–
Dunites	23	2.77	–
Olivine gabbro	55	2.65	–
Gabbro-norite	36	2.22	–

<sup>a</sup> Compiled using data from (Birch et al. 1942; Dakhnov and Dyakonov 1952; Lubimova et al. 1964; Magnitsky 1965; Clark 1966; Lubimova 1968b; Dmitriev et al. 1969; Aliev and Mekhtiev 1970; Kutas and Gordienko 1971; Mekhtiev et al. 1971, 1972, 1973; Starikova and Lubimova 1973; Lubimova and Smirnova 1974; Aliev et al. 1977; Zinger and Kotrovsky 1979; Gillis et al. 1993; Cannat et al. 1995; Kelemen et al. 2004)

conductivity values. The average heat conductivity of gabbro from the Mid-Atlantic ridge is 2.20 W/(m K) (calculated using data from Cannat et al. 1995; Kelemen et al. 2004), but its value from the East Pacific Rise is 2.58 W/(m K) (calculated using data from Gillis et al. 1993).

Such discrepancies prove that it is wise to use data obtained from local rocks to conduct geothermal calculations and analyze the geothermal regime of a region, since applying published average values not related specifically to the rocks and conditions of the target area can clearly lead to significant error.

## 2.2 Thermal Capacity

This parameter is defined as the amount of energy required to raise the temperature of a unit of the mass of a substance by 1°. The specific heat indicates the capability of the formations to store heat. The dimension of specific heat in the SI is: J/kg K.

The specific heat can be measured at constant pressure ( $c_p$ ) or at constant volume ( $c_v$ ). For an incompressible material the specific heats are equal to one another,  $c(T) = c_p(T) = c_v(T)$ . The  $c(T)$  is a weak function of the temperature and for a wide temperature interval it can be approximated by a linear equation,

$$c(T) = c(T_i) + \beta(T - T_i), \quad (2.2.1)$$

where  $T_i$  is the initial temperature, and  $\beta$  is the coefficient.

From experimental data (Somerton 1958) we calculated parameters in Eq. (2.2.1) for several rocks. For the 70 °F (21 °C)–620 °F (327 °C) interval we obtained the following values for sandstone  $c(70\text{ °F}) = 0.197\text{ Btu/lbm}^{-1}\text{ °F}^{-1}$  and  $\beta = 1.24 \times 10^{-4}\text{ Btu lbm}^{-1}\text{ °F}^{-2}$ . The corresponding values of  $c(70\text{ °F})$  and  $\beta$  are: 0.190 and  $1.43 \times 10^{-4}$  for shale; and 0.203 and  $1.12 \times 10^{-4}$  for siltstone. Very often a density and specific heat product ( $\rho c$ )—volumetric heat capacity is used. For fluid-saturated rocks at high temperatures the effective specific heat of the reservoir ( $c_R$ ) can be estimated from the following equations (Prats 1982):

$$c_R = \frac{M_R}{\rho_a} \quad (2.2.2)$$

$$\left\{ \begin{aligned} M_R &= (1 - \phi)M_\delta + \phi(S_oM_o + S_wM_w) + \phi S_g \\ &\times \left[ fM_g + (1 - f) \left( \frac{\rho_s L_v}{\Delta T} + \rho_s C_w \right) \right], \quad \Delta T = 1\text{ °C} \end{aligned} \right\}, \quad (2.2.3)$$

$$\rho_a = \rho_\delta(1 - \phi) + \phi(S_o\rho_o + S_w\rho_w + S_g\rho_g), \quad (2.2.4)$$

where  $\rho_a$  is the average density,  $M_R$  is the effective volumetric capacity,  $\phi$  is porosity,  $f$  is the volume fraction of non-condensable gas in the vapor phase;  $M_\delta$ ,  $M_o$ ,  $M_w$ , and  $M_g$  are the isobaric volumetric heat capacities of the solid, oil, water, and gas respectively;  $S_o$ ,  $S_w$  and  $S_g$  are the saturation of the fluid and gas phases;  $L_v$  is the latent heat of vaporization of water;  $c_w$  is the isobaric specific heat capacity of water;  $\rho_s$  is the steam density,  $\rho_\delta$ ,  $\rho_o$ ,  $\rho_w$  and  $\rho_g$  are the densities of the solid, oil, water, and gas phases, respectively.

Some values of the thermal capacity of typical formations have been presented in the literature (Kappelmeyer and Hänel 1974; Proselkov 1975; Somerton 1992). Some thermal properties after Proselkov (1975) are presented in Tables 2.6, 2.7.

The average values of specific heat capacity ( $c$ ) for certain rocks are presented in Tables 2.8 and 2.9. Published data were used to compile Table 2.8 (Birch et al. 1942; Dakhnov and Dyakonov 1952; Lubimova et al. 1964; Magnitsky 1965; Clark 1966; Lubimova 1968b; Dmitriev et al. 1969; Aliev and Mekhtiev 1970;

**Table 2.6** Thermal properties of rocks in the Romashkino oil field (Russia), after Proselkov (1975)

Formation	$\rho \times 10^{-3}$ (kg/m <sup>3</sup> )	$a \times 10^7$ (m <sup>2</sup> /s)	$\lambda$ [W/(m °C)]	$c \times 10^{-3}$ (J/kg °C)
Dolomite	2.75	9.95	2.11	0.802
Limestone	2.70	9.6	2.2	0.851
Clayey limestone	2.65	9.05	1.96	0.844
Argillite	2.3	9.94	2.25	0.838
Siltstone	2.55	10.8	2.22	0.795
Siltstone, oil-bearing	2.3	12.9	2.8	0.88
Clayey sandstone	2.5	14.3	3.36	0.915
Sandstone, fine-grained	2.55	7.19	1.55	0.844
Sandstone, fine-grained	2.4	10.5	1.85	0.845
Sandstone, oil-bearing	2.09	12.54	2.28	0.876
Sandstone, oil saturated	2.2	11.57	1.7	0.737
Sandstone, water saturated	2.3	12.8	2.46	0.84

**Table 2.7** Thermal properties of rocks (average data), after Proselkov (1975)

Formation	$\rho \times 10^{-3}$ (kg/m <sup>3</sup> )	$a \times 10^7$ (m <sup>2</sup> /s)	$\lambda$ (W/m °C)	$c \times 10^{-3}$ (J/kg °C)
Chalk	1.810	4.73	0.82	0.959
Chalk, compacted	1.920	5.80	1.02	0.922
Marl	1.970	4.04	1.38	1.734
Dolomite	2.753	9.95	2.11	0.802
Clayey limestone	2.644	9.05	1.96	0.844
Limestone	2.714	9.60	2.20	0.851
Clay	2.080	3.21	1.42	2.127
Sandy shale	2.057	3.21	1.42	2.151
Argillite	2.555	9.94	2.25	0.838
Sandstone, oil-bearing	2.198	11.57	1.70	0.737
Clayey siltstone	2.566	10.80	2.22	0.795
Quartzite schist	2.710	18.00	4.19	0.858

Kutas and Gordienko 1971; Mekhtiev et al. 1971, 1972, 1973; Starikova and Lubimova 1973; Lubimova and Smirnova 1974; Aliev et al. 1977; Zinger and Kotrovsky 1979).

Schärli and Rybach (2001) reported values of specific heat  $c_p$  of 752 J/(kg K) for granodiorite, 775 J/(kg K) for diorite, 720 J/(kg K) for granite, and 827–855 J/(kg K) for peridotite.

## 2.3 Thermal Diffusivity

Under transient conditions this parameter determines how fast the temperature field of a solid changes with time. The coefficient of thermal diffusivity ( $a$ ) is expressed by the formula



**Table 2.8** Average values of specific heat capacity [ $c$  in  $10^{-3}$  J/(kg K)] for some rocks

Rock	N	$c$
Sand	130	0.96
Siltstone	42	0.87
Argillite, clay schist	18	0.86
Clay	116	1.10
Marl	19	1.55
Limestone	108	0.89
Chock	13	1.86
Granite	87	0.95
Granodiorite	11	1.02
Porpyrite	11	0.91
Diorite	4	1.00
Basalt	12	1.23
Diabas	12	0.87
Gabbro	13	0.98
Schist	95	1.10
Gneiss	14	1.02
Amphibolite	7	1.13
Gneiss-granite	15	1.11

**Table 2.9** Average values of specific heat capacity [ $c$  in  $10^{-3}$  J/(kg K)] for some rocks (after ETB 2011)

Rock, mineral	Specific heat capacity ( $C_p$ ) [kJ/(kg K)]
Augite	0.8
Basalt rock	0.84
Dolomite rock	0.92
Garnet	0.75
Granite	0.79
Hornblende	0.84
Hypersthene	0.8
Labradorite	0.8
Lava	0.84
Limestone	0.84
Sand	0.8
Sandstone	0.92
Serpentine	1.09

$$a = \frac{\lambda}{\rho c}. \quad (2.3.1)$$

The dimension of thermal diffusivity is  $\text{m}^2/\text{s}$ . In hydrodynamics, the analogous quantity is hydraulic diffusivity (the ratio of mobility to the product of porosity and total system compressibility). Some values of the thermal properties of certain formations have been presented in the literature (Birch and Clark 1940; Clark 1966; Kappelmeyer and Hänel 1974 (Table 2.10); Somerton 1992).

The average values of thermal diffusivity ( $a$ ) for certain rocks are listed in Table 2.11 from published data (Birch et al. 1942; Dakhnov and Dyakonov 1952;

**Table 2.10** Thermal properties of sedimentary rocks at temperature of 50 °C (Kappelmeyer and Hänel 1974)

Material	$n$	$\rho, \rho_{\text{aver}}$ (g/cm <sup>3</sup> )	$\lambda, \lambda_{\text{aver}}$ (10 <sup>-3</sup> cal/cm s °C)	$n$	$c, c_{\text{aver}}$ (cal/g °C)	$a, a_{\text{aver}}$ (10 <sup>-3</sup> cm <sup>2</sup> /s)
Anhydrite	7	2.65–2.91 2.80	9.80–14.50 12.61	7	– –	17.00–25.7 22.41
Clay	3	2.49–2.54 2.52	5.20–5.40 5.30	3	0.213–0.240 0.223	8.53–10.18 9.50
Clay marl	7	2.43–2.64 2.54	4.14–6.15 4.87	7	0.186–0.234 0.205	8.01–11.66 9.34
Claystone	15	2.36–2.83 2.60	4.17–8.18 5.68	9	0.197–0.223 0.211	8.24–15.80 12.18
Dolomite	6	2.53–2.72 2.63	6.01–9.06 7.98	6	0.220–0.239 0.228	10.75–14.97 11.17
Schistose clay	3	2.42–2.57 2.49	4.60–5.50 5.13	3	0.218–0.222 0.220	8.10–10.24 9.37
Limestone	11	2.41–2.67 2.55	4.05–6.40 5.28		0.197–0.227 0.204	8.24–12.15 10.54
Limestone	6	2.58–2.66 2.62	5.58–8.38 6.75	6	0.197–0.220 0.210	10.78–15.21 12.18
Lime marl	2	2.43–2.62 2.53	4.40–5.74 5.07	2	0.200–0.227 0.214	9.04–9.64 9.34
Marl	3	2.59–2.67 2.63	5.55–7.71 6.44	3	0.217–0.221 0.219	9.89–13.82 11.18
Marly clay	2	2.46–2.49 2.47	4.21–4.82 4.52	3	0.183–0.236 0.210	7.17–10.72 8.94
Clay slate		2.62–2.83 2.68	3.45–8.79 5.13	5	0.205–0.205 0.205	6.42–15.15 9.26
Salt	5	2.08–2.28 2.16	10.7–13.7 13.19	14	– –	25.20–33.80 30.60
Salt slate	14	2.13–2.57 2.37	3.00–10.00 6.59	7	– –	6.38–21.70 13.90
Sandstone	7	2.35–2.97 2.65	5.20–12.18 7.75	31	0.182–0.256 0.197	10.94–23.62 16.45

Lubimova et al. 1964; Magnitsky 1965; Clark 1966; Lubimova 1968b; Dmitriev et al. 1969; Aliev and Mekhtiev 1970; Kutas and Gordienko 1971; Mekhtiev et al. 1971, 1972, 1973; Starikova and Lubimova 1973; Lubimova and Smirnova 1974; Aliev et al. 1977; Zinger and Kotrovsky 1979).

## 2.4 Melting Points of Rocks and Minerals

The melting point of a substance is the temperature at which the solid and liquid phases exist in equilibrium and the substance can be transformed from one of these states into the other. Transformations of one state to another are known as the

**Table 2.11** Average values of thermal diffusivity ( $a$ , in  $10^{-7} \text{ m}^2/\text{s}$ ) for some rocks

Rock	$N$	$a$
Sand	154	9.57
Siltstone	45	10.28
Argillite, clay schist	23	9.76
Clay	126	7.30
Marl	26	7.53
Limestone	115	10.92
Chock	13	4.77
Granite	92	9.13
Granodiorite	16	5.15
Porpyrite	23	9.54
Diorite	10	6.38
Basalt	13	5.34
Diabas	13	9.93
Gabbro	21	9.70
Schist	106	9.60
Gneiss	15	7.98
Amphibolite	9	6.84
Gneiss–granite	18	7.24

fusion point, freezing point or crystallization point. The melting point of rocks and minerals is an extremely important feature because it characterizes the temperature at which different rocks and minerals change from a solid to a liquid and back. The process of melting and solidification of rocks and minerals can also be defined by the liquids and solidus temperatures of a substance, which together with the melting point are fundamental physical properties of every rock and mineral. The solidus temperature is the temperature (or curve on a phase diagram) below which a substance is completely solid. It quantifies the temperature at which the melting of a substance begins, while not yet completely melted. Conversely, the liquidus temperature is the temperature at which a substance is completely melted and homogeneous. No crystals can exist within the substance above this temperature. Similarly, below the liquidus temperature the crystallization of a substance begins while it is not yet completely solid.

Merely reaching the melting point temperature does not guarantee that the substance will begin melting, since the melting process requires additional heat energy to convert it from a solid to a liquid state. The amount of additional energy needed is termed the *latent heat of fusion*; i.e., the amount of energy absorbed by a substance during a change of state from a solid to a liquid. In the case of the solidification of a melt, the latent heat of fusion (crystallization) represents the amount of heat released during the conversion of the melt to a solid state at the melting point. The latent heat of fusion is also a characteristic physical parameter that varies for different rocks and minerals.

Thus, overall, the melting point, the solidus and liquidus temperatures, and the latent heat of fusion are parameters expressing the heat energy of rock and/or

**Table 2.12** Melting points of some rock-forming minerals

Mineral	Melting point (K)	References
Fayalite	1,490	Hewins et al. (1996)
Fayalite	1,478	Yoder (1976)
Forsterite	2,163	Hewins et al. (1996)
Forsterite	2,163	Yoder (1976)
Forsterite	2,171	Speight (2005)
Enstatite	1,830	Speight (2005)
Clinoenstatite	1,830	Hewins et al. (1996)
Ferrosilite	1,413	Speight (2005)
Albite	1,391	Hewins et al. (1996)
Albite	1,393	Hall (1995)
Anorthite	1,830	Hewins et al. (1996)
Christobalite	1,996	Hewins et al. (1996)
Diopside	1,664	Hewins et al. (1996)
Diopside	1,665	Wenk and Bulakh (2004)
Fe metal	1,889	Hewins et al. (1996)
Wollastonite	1,813	Nikonova et al. (2003)
Augite	1,440–1,455	Thy et al. (1999)
Low-Ca pyroxene	1,386–1,426	Thy et al. (1999)
Olivine (Fo82)	1,955	Del Gaudio et al. (2009)
Olivine (Fo85)	1,993	Del Gaudio et al. (2009)
Pyrope	1,575–1,609	Van Westrenen et al. (2001)
Pyrope	1,570	Téqui et al. (1991)
K-feldspar	1,423	Best (2002)
Pure leucite	1,958	Best (2002)

mineral at the temperature when it transforms from a solid to a liquid or vice versa. These parameters are crucial for analyzing the heat capacity and level of heat transfer during the formation of magma, the uplift of magma to the surface, magma eruption, and other related processes. The melting point of different rocks and minerals is important for estimating the amount of heat energy contained within the magma-ocean, the amounts released during differentiation and solidification of the magma-ocean, the rates of cooling of different layers of the magma-ocean, the amounts of heat energy needed to form magma chambers within solid crustal layers, the amount of heat transferred by erupting magma, etc. The melting point can also reveal which mineral would be first to solidify within the magma-ocean and in what sequence others would follow within its different layers or magma chambers. The melting points of some key minerals and rocks are presented in Tables 2.12 and 2.13.

Note that the melting point of any rock or mineral increase with increases in pressure, and therefore with depth. See for example Table 2.14.

On the other hand, it is well-known that the melting point of rocks and minerals drops significantly with increases in water, carbon dioxide or iron content. For instance, at a depth of about 100 km, peridotite begins to melt at a temperature of

**Table 2.13** Melting points of some rocks

Rock	Melting point (K)	References
Basalts	~1,473	Adylov and Mansurova (1999)
Basic rocks with Fe# = 0.35	~1723	Yoder (1976)
Basic rocks with Fe# = 0.50	~1,503	Yoder (1976)
Basic rocks with Fe# = 1.00	1,273	Yoder (1976)
Basalt (beginning of melting at 0.1 MPa)	1,273	Yoder (1976)
Basalt	1,343	Hall (1995)
Basalt	1,413	Hall (1995)
Basalts	1,473	Faure (2000)
Basalt, gabbro	1,473	Bayly (1968)
Rhyolite, granite	1,073	Bayly (1968)
Granites	973–1,123	Attrill and Gibb (2003)
Granite	1,173	Hall (1995)
Granite	1,223	Hall (1995)
Komatiites	2,063	Grove and Parman (2004)
Andesite	1,373	Tamura et al. (2003)
Andesite	1,343	Hall (1995)
Eclogite	1,573	Anderson (2007)
Tonalite	1,173	Hall (1995)
Tholeiitic basalt <sup>a</sup>	1,423–1,498	Hall (1995)
Basaltic andesite <sup>a</sup>	1,293–1,383	Hall (1995)
Leucite basalt <sup>a</sup>	1,368	Hall (1995)
Rhyolite <sup>a</sup>	1,008–1,163	Hall (1995)
Rhyodacite <sup>a</sup>	1,173–1,198	Hall (1995)
Andesite pamice <sup>a</sup>	1,213–1,263	Hall (1995)
Dacite <sup>a</sup>	1,198	Hall (1995)
Peridotite	1,363	Faure and Mensing (2007)
MORB <sup>a</sup>	1,516–1,624	Falloon et al. (2007)
OIB <sup>a</sup>	1,559–1,645	Falloon et al. (2007)

<sup>a</sup> Extrusion temperatures of lavas**Table 2.14** Melting point of peridotites at different pressures

Peridotite	Pressure (GPa)	Melting point (K)	References
	0	1,363	Faure and Mensing (2007)
Dry peridotite	~3	1,613	Faure and Mensing (2007)
	~13.2	1,973	Faure and Mensing (2007)
	1	1,483	Lee et al. (2009)
Dry lherzolite solidus	~3	1,713	Lee et al. (2009)
	~6	1,973	Lee et al. (2009)
Dry peridotite	0	1,400	Schubert et al. (2001)
	~3	1,700	Schubert et al. (2001)

about 1,073 K with the presence of excess water, but at the same depth, dry peridotite will start melting at about 1,773 K (Grove et al. 2006). The solidus temperature of lherzolite containing 5 % water is about 1,273 K at ~0.5 GPa, and

about 1,653 K at  $\sim 4$  GPa (Lee et al. 2009). However, the solidus temperature of lherzolite containing 10 % water is about 1,273 K at 1.25 GPa, and about 1,543 K at  $\sim 4$  GPa (Lee et al. 2009). At standard pressure, peridotites melt at temperatures of  $\sim 1,400$  K in the absence of water and other volatiles, and their solidus increases with pressure to around 1,700 K at  $\sim 3$  GPa (Schubert et al. 2001). However, even concentrations of  $\text{H}_2\text{O}$  as low as only 0.1 % reduce the standard pressure melting point to  $\sim 1,340$  K, and it actually continues to decrease with pressure, reaching a minimum near 1,270 K at about 3 GPa (Schubert et al. 2001). At higher pressures and greater water content, the melting point of peridotite can drop by about 300–400 K (Schubert et al. 2001).

Experiments document that in the presence of carbon dioxide, the peridotite solidus temperature decreases by  $\sim 200$  K at a depth of about 70 km, whereas at greater depths the carbon dioxide present can reduce the initial melting temperatures of a carbonated peridotite by about 450–600 K compared to the same composition devoid of carbon dioxide (Dasgupta and Hirschmann 2007). Schubert et al. (2001) also indicated that the presence of  $\text{CO}_2$  lowers the melting point.

Lastly, the increase of iron content also significantly lowers the melting point of silicates (Kushiro et al. 1968; McCall 1973; Pilchin and Eppelbaum 2004, 2006). We can see this by comparing the melting points of Mg-rich to Fe-rich olivines (forsterite and fayalite) to orthopyroxenes (enstatite and ferrosilite). See Table 2.12, which reveals this trend.

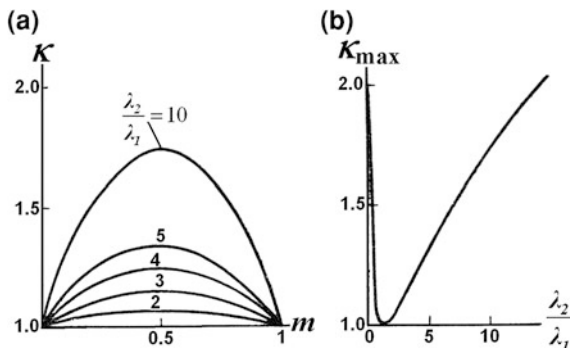
## 2.5 Effect of Thermal Anisotropy

The term “anisotropy” can be defined as an observed difference when measurements are made on different axes of a given material (in our case geological rock). The thermal anisotropic properties of graphitic, coal, pyritized and other shale, stratified clays and sandstone, some types of sulphide ores, igneous (for instance, xenoliths) and metamorphic rocks were identified some years ago (Lubimova 1968a, b; Cheremensky 1977; Brigaud 1989; Clauser and Huenges 1995). Simmons (1961) underlined that the thermal conductivity calculated in a single borehole through anisotropic rock will not correspond to the thermal conductivity parallel to the borehole.

Clauser and Huenges (1995) suggested the following three-tier classification:

1. Anisotropic of minerals (microscopic scale),
2. Anisotropy of rocks (laboratory scale). However, even if rocks are composed of anisotropic minerals, the common random orientation of the crystals within the rock may affect the rock's thermal conductivity isotropically,
3. Anisotropy of rock complexes (areal or regional scale). Tectonic processes such as folding, orogeny, displacement etc., the thermal conductivity of the resulting rock formation may be either isotropic as or anisotropic.

**Fig. 2.3** Relationships: **a** between the coefficient of thermal anisotropy  $\kappa$  and parameter  $m$ , **b** between the maximal value of  $\kappa$  and ratio  $\lambda_2/\lambda_1$  (after Cheremensky 1977)



It should be noted that methods of anisotropy calculation have been studied in detail in electric prospecting (e.g., Dakhnov 1972) which makes it possible to transfer the obtained solution (with necessary modifications) to thermal data analysis.

In a first approximation, anisotropic rock may be present as two-component medium consisting of interbedding of alternations with a thickness of  $h_1$  and  $h_2$  and thermal conductivities  $\lambda_1$  and  $\lambda_2$ . Thus we can calculate a coefficient of thermal anisotropy  $\kappa$ :

$$\kappa = \sqrt{\frac{\lambda_T}{\lambda_n}} = \sqrt{1 + \frac{m(1-m)(\lambda_1 - \lambda_2)^2}{\lambda_1 \lambda_2}}, \quad m = \frac{h_1}{h_1 + h_2}, \quad (2.5.1)$$

where  $\lambda_T$  and  $\lambda_n$  are the longitudinal ( $\parallel$ ) and transversal ( $\perp$ ) thermal conductivities, respectively. In any case  $\lambda_T \geq \lambda_n$ . The value of  $\kappa$  increases with increasing number of alterations and reaches its maximum value by  $m = 0.5$  (Fig. 2.3). The relation  $\lambda_T/\lambda_n$  for claystone and limestone of Donbas (Ukraine) were found to be 1.6 and 1.4, respectively (Kutas and Gordienko 1971). Popov et al. (2003) described the significant effect of thermal anisotropy of sedimentary rocks on other physical parameters and underlined the advantage of using the component  $\lambda_T$ .

## 2.6 Effect of Temperature and Pressure on the Thermal Properties of Rocks and Minerals

Analysis of experimental data on the variance of thermal parameters with increases in temperature and pressure shows that in general, heat conductivity ( $\lambda$ ) declines, heat capacity ( $C_p$ ) increases and thermal diffusivity ( $a$ ) decreases considerably with increases in temperature. Stated differently, at low and moderate temperatures (up to 573–773 K) the value of heat conductivity varies proportionally with the reciprocal of the temperature (Lubimova 1968b; Clauser and Huenges 1995, amongst others), but the actual relationships between these two

parameters are more complicated. For example, Eucken's empirical law (1911) shows that the thermal resistivity ( $1/\lambda_1$ ) of a crystalline dielectric at  $T \geq \theta$  is directly proportional to its absolute temperature (Petrudin and Popov 1995):

$$\frac{1}{\lambda_1} = \text{const} \cdot T, \quad (2.6.1)$$

which can be described by the equation (Litovsky and Shapiro 1992):

$$\lambda = (C + DT)^{-1}, \quad (2.6.2)$$

where  $C$  and  $D$  are the material-dependent constants.

To determine the thermal conductivity of most rocks in the upper crust, Čermak and Rybach (1982) used the equation:

$$\lambda = \frac{\lambda_0}{1 + cT}, \quad (2.6.3)$$

where  $\lambda_0$  is the thermal conductivity at 0 °C (273.15 K) and near-surface pressure conditions, and  $c$  is a material constant (in the range of 0–0.003 °C<sup>-1</sup>) determined through experimental studies on rock samples (for the actual study,  $c$  was assumed to be 0.001 °C<sup>-1</sup> for the upper crust).

Zoth and Hänel (1988) suggested that a relationship existed of the form:

$$\lambda(T) = A + \frac{B}{350 + T}, \quad (2.6.4)$$

where  $\lambda$  is given in W/(m K),  $T$  in °C, and the empirical constants  $A$  and  $B$  are determined from a least-squares plot of measured data for different rock types.

Experimental research on the dependence of heat conductivity on temperature by Vosteen and Schellschmidt (2003) showed that the mean values of  $\lambda$  drop for magmatic, metamorphic, and sedimentary rocks from 2.4, 2.6 and 2.75 Wm<sup>-1</sup> K<sup>-1</sup> respectively at 273 K, to 1.5, 1.4, and 1.6 Wm<sup>-1</sup> K<sup>-1</sup> respectively at 573 K. Other studies have shown (Clark 1966) that at a temperature of 473 K, the values for granite, tonalite, and syenite can drop to as low as 2.14, 2.31, and 2.09 Wm<sup>-1</sup> K<sup>-1</sup>, respectively. For sedimentary rocks at temperatures of up to 573 K, there is a reduction of heat conductivity by nearly a factor of two (Clauser 2006, 2009). For quartzite this decline is very rapid, by nearly a factor of three up to a temperature of ~773 K (Clauser 2009). There are some reports (Clauser and Huenges 1995; Clauser 2009) that at high temperatures the radiative component of heat conductivity appears and balances and in some cases even inverts the decreasing trend of heat conductivity with the increase in temperature at about 1,273–1,473 K. Clauser and Huenges (1995) showed that with increases in temperature up to 573 K, there is a reduction of heat conductivity by nearly a factor of two for both clastic and carbonaceous sediments, while above 573 K the decrease is much slower. They also noted that the heat conductivity of volcanic rocks decreases to about 1,173 K, at which point it is about 50 % of its value at ambient temperature, and that at temperatures



above 1,073–1,273 K the radiative component of thermal conductivity starts to rise, although they did not find a very significant radiative contribution in plutonic rocks.

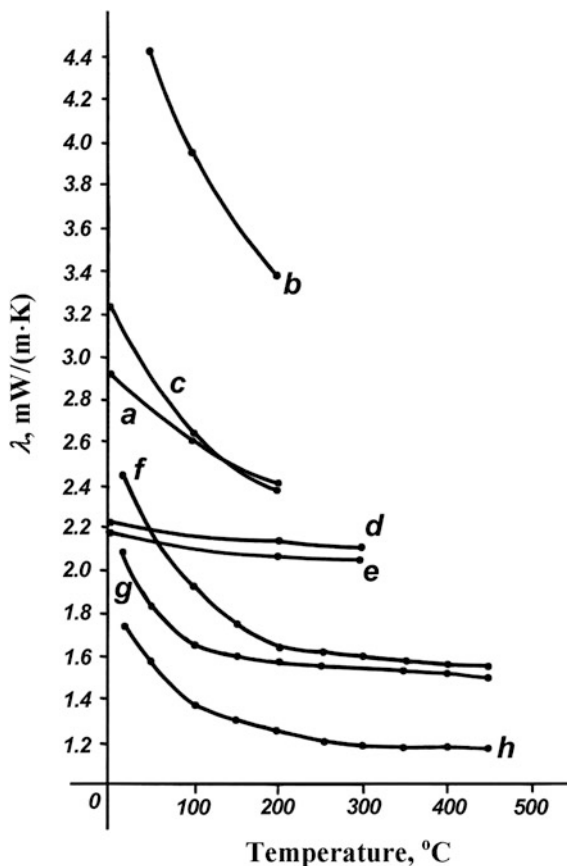
At the same time, radiation only becomes a very efficient form of heat transfer above 1,473 K (Clauser 2006). Ray et al. (2008) stated that in granulites, the radiative heat transfer is negligible up to 823 K. Similarly, Kukkonen et al. (1999) failed to find a radiative heat-transfer effect to be present below 1,150 K for mafic granulites. Aronson et al. (1970) also showed that opacity significantly decreases the magnitude of radiative thermal conductivity. Another study demonstrated that radiation is more effective for rocks with a larger mean free path of radiation corresponding to smaller values of their absorption coefficient and opacity (Clauser 1988, 2006). For metamorphic rocks, the heat conductivity at  $\sim 473$  K decreases by about 33 % of its value at ambient temperature, and then drops again by about an additional 33 % of its value at ambient temperature with increases in temperature to  $\sim 1,023$  K (Clauser and Huenges 1995). Pribnow et al. (1996) showed that the thermal conductivity of water-saturated rocks from the KTB Pilot Hole took longer to decline with increasing temperatures than dry rocks. Differences in heat conductivity with increases in temperature for some typical rocks are presented in Fig. 2.4.

Research (Vosteen and Schellschmidt 2003) showed that the mean values and ranges of the variable specific heat capacity  $c_p$  at constant pressure for magmatic, metamorphic, and sedimentary rocks increases respectively from about 760, 770 and 810 J kg<sup>-1</sup> K<sup>-1</sup> at 273 K, to about 970, 970, and 1,010 J kg<sup>-1</sup> K<sup>-1</sup> at 573 K. Sometimes parameters such as the thermal capacity ( $\sigma \cdot C_p$ , where  $\sigma$  is the density) are used to characterize the thermal properties of rocks and minerals. However, since the thermal volume expansion coefficient of rocks and minerals is very small (on the order of  $\sim 10^{-5}$  K<sup>-1</sup>), the variable density with increases in temperature will also be extremely insubstantial and so may be ignored. The value of density can therefore be accepted as a constant (Vosteen and Schellschmidt 2003).

The thermal diffusivity, which describes the equilibration of a temperature imbalance, is a function of thermal conductivity  $\lambda$ , density  $\sigma$ , and specific heat capacity  $C_p$  at a constant pressure:  $a = \frac{\lambda}{\sigma C_p}$ . The temperature-dependence of thermal diffusivity is usually proportional to the reciprocal of the absolute temperature (Seipold and Gutzeit 1980). Given that with temperature increasing, the thermal conductivity decreases, the specific heat capacity increases whereas the density does not change significantly. Thus it is clear from the definition of thermal diffusivity that it will decline sharply with temperature increasing. In reality, experimental data on variable thermal parameter values with increase of temperature show that for magmatic, metamorphic, and sedimentary rocks within a temperature interval of 273–573 K, the thermal conductivity decreases by 25–44 % and the thermal diffusivity decreases by 42–54 %.

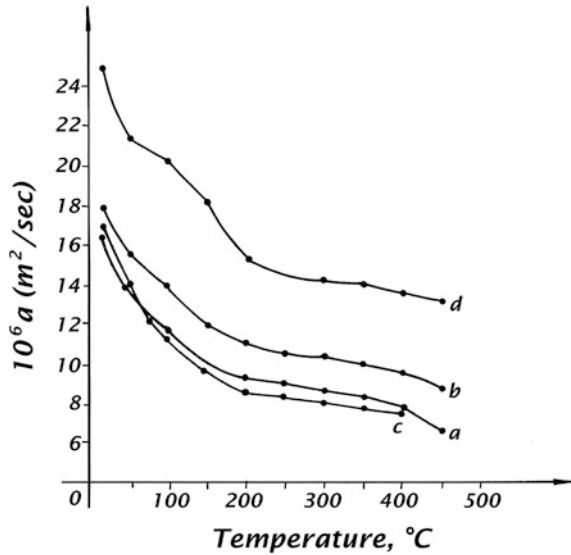
Thermal diffusivity (in mm<sup>2</sup>/s) for all the rocks investigated in Whittington et al. (2009) went from  $\sim 1.8$ –2.2 at  $\sim 298$  K to  $\sim 0.3$ –0.5 at 1,200–1,250 K. They also provide data demonstrating that it drops substantially from 1.5–2.5 mm<sup>2</sup>/s at ambient conditions to about 0.5 mm<sup>2</sup>/s at mid-crustal temperatures which goes to

**Fig. 2.4** Variable heat conductivity with increases in temperature for some rocks: *a* and *h* granites; *b* dunite; *c* limestone; *d* and *g* diabase; *e* and *f* gabbro [data for samples *a*, *b*, *c*, *d*, and *e* taken from Clark (1966); and for samples *f*, *g* and *h* taken from Dmitriev et al. (1969)]



show that the hot middle-lower crust is a very effective thermal insulator. Ray et al. (2008) reported a decrease of the thermal diffusivity of granulites and amphibolite facies gneisses of about 35–45 % with temperature increasing from 293 to 723 K. Analysis of the thermal diffusivity of rocks of different origin shows that the value varies inversely with temperature, and is 50–75 % lower at 800 K than at ambient temperature (Hanley et al. 1978). At the same time, research shows that at ambient temperature rocks saturated with water have their thermal diffusivity increased by as much as 24 % (Hanley et al. 1978). Pertermann and Hofmeister (2006) reported results showing that the substitution of  $\sim 10$  % Fe for Mg in forsterite lowers the thermal diffusivity ( $\alpha$ ) by  $\sim 50$  %, and that the  $\alpha$  of olivines and olivine-rich rocks can decrease to about 20 % of its value at ambient temperature at 1,163–1,353 K. Hofmeister and Pertermann (2008) stated that thermal diffusivity decreases with increasing temperature, and approaches a constant at about 1,400 K. Their research also shows that for clinopyroxenes it decreases from  $\sim 3.9$  mm<sup>2</sup>/s at 298 K to about 0.5–0.9 mm<sup>2</sup>/s at  $\sim 1,400$  K. The variable thermal diffusivity with increase of temperature for some typical rocks is presented in Fig. 2.5.

**Fig. 2.5** Variable thermal diffusivity with increases in temperature for some rocks: *a* gabbro; *b* diabase; *c* granite; *d* granite-gneiss [using data from Dmitriev et al. (1969)]



Though its effect is much weaker than increases in temperature, increases in pressure lead to a general increase in heat conductivity as well. Clark (1966) also pointed out this weak influence of pressure on heat conductivity. Clauser and Huenges (1995) showed that for granite and metamorphic rocks, there is about a 10 % increase in heat conductivity over the entire range of pressures from 0 to 500 MPa, but the increase is the greatest over the first 50 MPa. The effect of pressure on the value of heat conductivity is mostly dependent on fractures, micro-cracks and porosity (Clauser 2006). Depending on the volume of space within these features, heat conductivity can increase by up to 20 %, with an increase in pressure to  $\sim 15$  MPa; whereas a further increase in pressure to  $\sim 40$  MPa typically does not lead to a change in heat conductivity. However, when the pressure is increased from 50 to 500 MPa it will lead to an additional increase of  $\sim 10$  % (Clauser 2006). Seipold and Gutzeit (1980) showed that in many cases thermal conductivity increases linearly with rising pressure from a rate of around  $10^{-5}$ – $10^{-4}$  MPa $^{-1}$ . Linear relationships between thermal transfer parameters and pressure for pressures ranging from 50 to 1,000 MPa were reported for metamorphic rocks of the Saxonian Granulite Mountains with pressure coefficients of  $(0.75 \pm 0.35) \times 10^{-4}$  MPa $^{-1}$  for thermal conductivity and  $(0.61 \pm 0.22) \times 10^{-4}$  MPa $^{-1}$  for thermal diffusivity (Seipold and Huenges 1998; Seipold 2002).

At the same time, certain researchers have suggested that the effects of pressure on the heat capacities of solids can be neglected (Waples and Waples 2004). The estimated pressure derivatives for clinopyroxenes are  $\partial(\ln k)/\partial P = (4.2\text{--}4.7) \times 10^{-5}$  MPa $^{-1}$  (Hofmeister and Pertermann 2008).

Durham et al. (1987) reported results showing that diffusivity in all cases rose or remained steady with increasing confining pressure, and that the effect of pressure was the strongest with the lowest pressures and vanished between 10 and

**Table 2.15** Pressure derivatives of thermal conductivity for some minerals (after Hofmeister 2007)

Mineral	$P_{\max}$ (MPa)	$\lambda^{-1} \partial \lambda / \partial P$ ( $10^{-4} \text{ MPa}^{-1}$ )
$\text{Mg}_2\text{SiO}_4$	500	16.0
$\text{Mg}_{1.8}\text{Fe}_{0.2}\text{SiO}_4$	200	12.0
$\text{Mg}_{1.8}\text{Fe}_{0.2}\text{SiO}_4$	1,000	9.0–12.0
$\text{Mg}_{1.8}\text{Fe}_{0.2}\text{SiO}_4$	4,800	~4.8
$\text{Mg}_{1.8}\text{Fe}_{0.2}\text{SiO}_4$	5,600	6.0–7.0
$\text{Mg}_{1.8}\text{Fe}_{0.2}\text{SiO}_4$	5,600	5.0–6.0
$\text{Mg}_{1.8}\text{Fe}_{0.2}\text{SiO}_4$	8,300	3.2–3.8
$\text{Mg}_{1.8}\text{Fe}_{0.2}\text{SiO}_4$	9,000	5.5
$\text{Mg}_{1.8}\text{Fe}_{0.2}\text{SiO}_4$	10,000	4.4
$\text{Mg}_{0.85}\text{Fe}_{0.15}\text{O}_3$	5,600	7.0
MgO	5,000	2.0–4.0
MgO	1,200	5.0
Coesite	4,000	3.9
Coesite	5,600	1.4–4.4
$\text{Py}_{25}\text{Al}_{74}\text{Gr}_1$ (garnet)	8,300	4.6
$\text{NaAlSi}_2\text{O}_6$	3,000	4.6

100 MPa, depending on rock type. Analysis of the combined influence of pressure and temperature on the value of the heat conductivity of marl also showed that the role of temperature is dominant (Lubimova et al. 1978). The differences in relative values of heat conductivity with pressure for some minerals are presented in Table 2.15.

## 2.7 The Impact of High Pressures and Temperatures on Fluid Density in a Porous Space Within Rocks and Rock Layers

Of all the types of rocks in the upper crust, sedimentary rocks have the highest porosity value which can reach 45 % for some clays. For instance, the average porosity of sedimentary layers in Azerbaijan is about 25 %. Porosity is generally expressed by the porosity coefficient  $K_p$ , which is calculated as the ratio of porous volume to the total volume of rock. Porous space is usually filled with some fluid, in most cases water; but in some instances it can be filled with oil, gas, and their mixtures with water. Conversely, magmatic and metamorphic rocks usually have very low porosity unless they are located in layers with pressures under 15 MPa. Since in the great majority of cases the porous space of rock is filled with water, the normal porous pressure ( $P_0$ ), known as the hydrostatic pressure, is usually calculated using the equation:

$$P_0 = 0.1 H, \quad (2.7.1)$$

where  $H$  is depth in meters (m) and the normal hydrostatic pressure  $P_0$  is in 100 kPa.

Thermodynamic conditions ( $P$ - $T$ -conditions) regulate the density of porous fluid, and this can be used in some cases to determine and/or analyse the  $P$ - $T$ -conditions present within a rock or rock layer.

It is crucial to note that in crystalline rocks the porous volume is held by the crystalline lattice, whereas in sedimentary rocks it is held by fluid-filled pores and their thermodynamic conditions. In sedimentary layers, there are conditions that allow a porous fluid to move more or less freely through the porous space (sands, sandstones, limestones, etc.), as well as conditions preventing the fluid from moving freely within the pores (sediments capped by clays, salt or frozen layers; in clays most of water is bound to clay minerals).

Knowing the lithostatic pressure value is extremely important in any study of the  $P$ - $T$ -conditions of a porous fluid, since in most cases it is capable of squeezing some amount of porous fluid out of porous space, thereby reducing the space. A similar effect can take place in tectonically active regions when an external tectonic force (typically horizontal) can squeeze fluid out of porous space. This effect can cause the porous pressure to increase to the value of the lithostatic pressure to achieve an equilibrium (Pilchin 1983). Such a situation would definitely lead to the formation of pressures within a porous fluid that are greater than its hydrostatic value determined by Eq. (2.7.1), a condition usually called overpressure or abnormally high stratum pressure (AHSP). The presence of AHSP is an enormous problem for drilling wells in oil and gas fields. It should be noted that in some cases one of the hallmarks of AHSP is abnormally low porous pressures, which are usually found within the first few hundred meters from the surface, as well as in some cooling layers.

To analyze the density and/or volume of any fluid or any other matter under given  $P$ - $T$ -conditions, coefficients such as volume thermal expansion ( $\alpha$ ) and compressibility ( $\beta$ ) are usually employed:

$$\alpha = \frac{(\partial V / \partial T)_P}{V_0}, \quad (2.7.2)$$

$$\beta = \frac{(\partial V / \partial P)_T}{V_0}, \quad (2.7.3)$$

where  $V$  and  $V_0$  are volume and initial volume, respectively.

It was shown (Pilchin 1978a; Kerimov et al. 1980; Mekhtiev et al. 1982; Pilchin and Eppelbaum 2009) that the relationship between the primary thermodynamic parameters Pressure-Temperature-Volume ( $P$ - $T$ - $V$ ) for any type of matter, without any preconditions, can be described by the equation:

$$P = P_0 + \frac{\alpha}{\beta}(T - T_0) - \frac{1}{\beta} \frac{\Delta V}{V_0}, \quad (2.7.4)$$

where  $P$  is the real pressure,  $P_0$  is the lithostatic or hydrostatic pressure,  $T$  is temperature,  $T_0$  is the normal temperature (the normal temperature for matter is determined using the condition for the equilibrium line ( $V/V_0 = 1$ ), as shown in

**Fig. 2.6** Change in a unit of volume of water under a wide range of pressures and temperatures, calculated using data from Clark (1966)

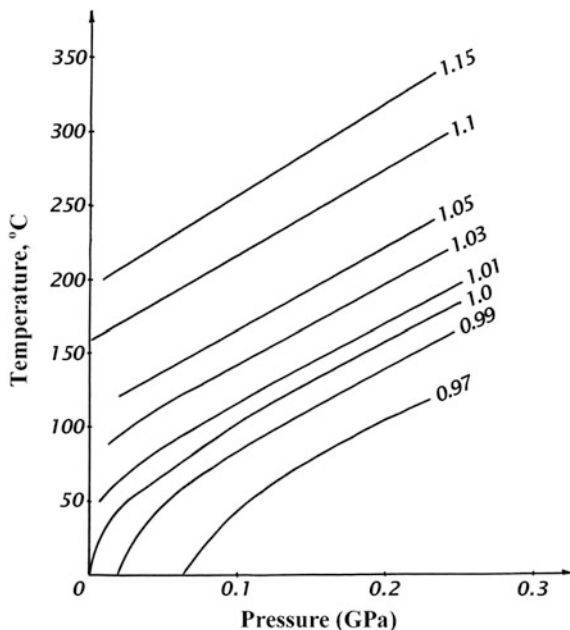


Fig. 2.6,  $\Delta V$  is the change in volume ( $V - V_0$ ), and  $V_0$  is the initial volume. The second term on the right side of the equation  $(\alpha/\beta)(T - T_0)$  characterizes the dependence of pressure on the temperature of the rock or rock layer. It is clear that temperatures greater than  $T_0$  will lead to an increase of pressure compared to the lithostatic or hydrostatic value, whereas temperatures lower than  $T_0$  will lead to pressures below the lithostatic or hydrostatic value. The third term on the right side of the equation  $(1/\beta) \cdot (\Delta V/V_0)$  represents pressure unloading (when  $\Delta V > 0$ ). This unloading can take place when some porous fluid is forced out by increasing porous pressure; for instance, by pumping out water, oil, or gas during well exploitation, etc. At the same time, there are possible cases where  $\Delta V < 0$ , which would lead to an increase in pressure and could represent such processes as tectonic compression. There are also possible scenarios where  $\Delta V = 0$ ; this represents a state of equilibrium and is used to determine the normal temperature  $T_0$ . For equilibrium conditions, Eq. (2.7.4) can be simplified into the following equation:

$$P = P_0 + \frac{\alpha}{\beta}(T - T_0). \quad (2.7.5)$$

A plot of the change in the volume unit of water ( $V/V_0$ ) with variable  $P$ - $T$ -conditions is presented in Fig. 2.6. The equilibrium condition  $\Delta V = 0$  is represented on the graph by the line  $V/V_0 = 1$ ; conditions with  $\Delta V > 0$  are represented by lines  $V/V_0 > 1$ , and  $\Delta V < 0$  are represented by lines  $V/V_0 < 1$  respectively.

It is clear from Eq. (2.7.5) that conditions of equilibrium can only be achieved when the real pressure is equal to its lithostatic or hydrostatic value. This is used to

determine the normal temperature ( $T_0$ ) for different types of matter, because a case of  $P = P_0$  necessarily has  $T = T_0$ . Calculating the lithostatic (Pilchin and Eppelbaum 2002, 2009) or hydrostatic pressure using Eq. (2.7.1) for different depths and substituting it for  $P_0$  in Eq. (2.7.5) can be used to find the value of the normal temperature  $T_0$  for the rock or mineral at the depth for which  $P_0$  was determined. It is clear that for each depth there is only one pair of  $P_0$  and  $T_0$  values, represented by the line of equilibrium ( $V/V_0 = 1$ ) in Fig. 2.6.

From the definition of the density  $\sigma$  of matter, which is its mass ( $m$ ) divided by its volume ( $V$ ) (or as the mass of a unit volume of matter), it is obvious that the condition of equilibrium  $\Delta V = 0$  results in:

$$\Delta\sigma = 0, \quad (2.7.6)$$

where  $\Delta\sigma = (\sigma - \sigma_0)$  is the change of density of the rock, mineral, etc.

Given the relationship between variable volume and variable density (e.g., Pilchin and Eppelbaum 2009):

$$\frac{\Delta V}{V_0} = -\frac{\Delta\sigma}{\sigma}. \quad (2.7.7)$$

Equation (2.7.4) can be rewritten as:

$$P = P_0 + \frac{\alpha}{\beta}(T - T_0) + \frac{1}{\beta} \frac{\Delta\sigma}{\sigma}. \quad (2.7.8)$$

Another important relationship between the relative change in volume and relative change in density is (Pilchin and Eppelbaum 2009):

$$\frac{\Delta V}{V_0} = -\frac{\Delta\sigma/\sigma_0}{(1 + \Delta\sigma/\sigma_0)}. \quad (2.7.9)$$

It should be pointed out that the values of the coefficients of volume heat expansion ( $\alpha$ ) and compressibility ( $\beta$ ) also depend on pressure and temperature, and these relationships are presented in Figs. 2.7 and 2.8.

These figures show that neither  $P_0$  nor  $T_0$  is constant, and that both are depth dependent parameters. This means that the relationship described by Eq. (2.7.4) indicates the dependence of pressure ( $P$ ) not on the temperature ( $T$ ), but rather on the excess temperature ( $T - T_0$ ). The use of the  $P_0$ ,  $T_0$  pairs for each depth thus provides an opportunity to use compatible and correlated values to analyze both pressure and temperature conditions simultaneously.

Another advantage of using both  $P_0$  and  $T_0$  in analyzing the thermodynamic conditions of porous fluids is the elimination of the dependence on depth of such parameters as  $K_{aP}$  (coefficient of abnormality of pressure defined as  $K_{aP} = P_{AHSP}/P_0$ ),  $K_{aT}$  (coefficient of abnormality of temperature defined as  $K_{aT} = T/T_0$ ), the excess of pressure ( $P - P_0$ ), the excess of temperature ( $T - T_0$ ), etc. (Kerimov and Pilchin 1986b). In fact, both the excess of pressure and the excess of temperature could have the same values at different depths, which would obviously produce different effects and create problems in interpreting these values together. In order to avoid such problems, it was suggested (Pilchin 1983; Kerimov and Pilchin

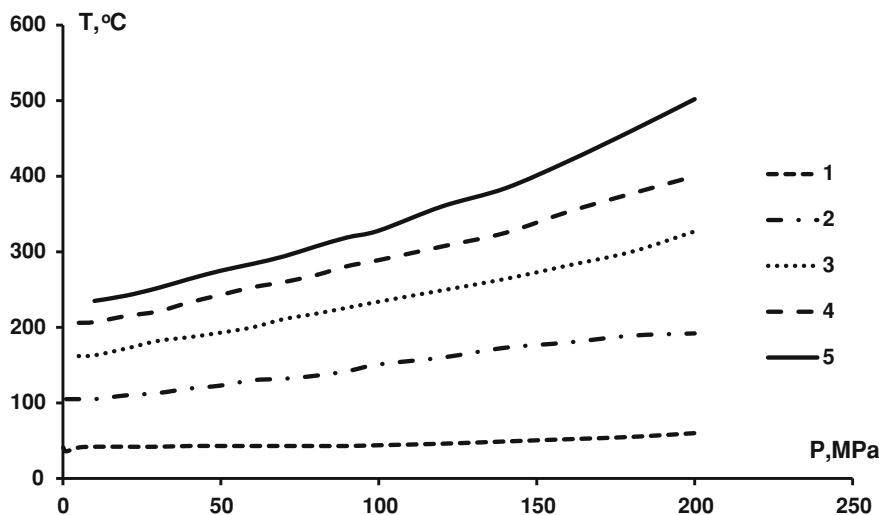
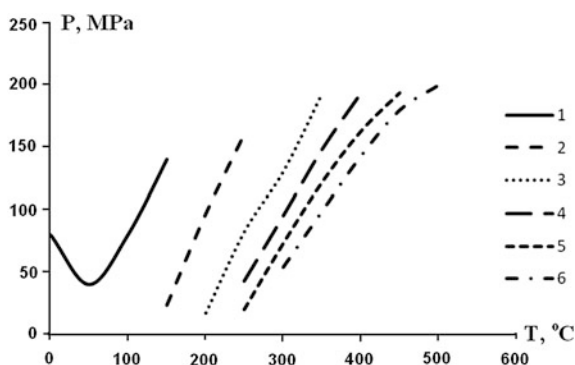


**Fig. 2.7** Changes in the coefficient of volume expansion of water ( $10^4 \times \alpha$ ,  $1/^\circ\text{C}$ ) under a wide range of pressures and temperatures, calculated using data from Clark (1966)

**Fig. 2.8** Changes in the coefficient of compressibility of water [ $10^5 \times \beta$ ,  $1/(10^2 \text{ kPa})$ ] under a wide range of pressures and temperatures, calculated using data from Clark (1966)

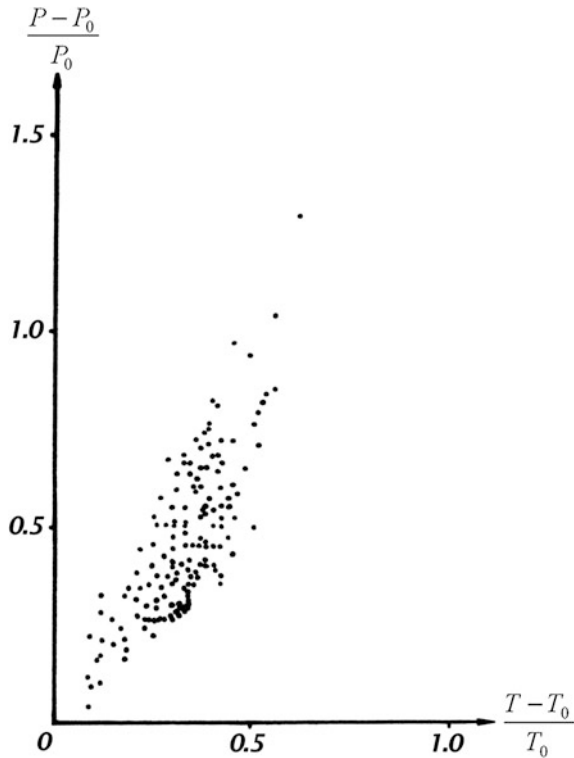


1986b) to use dimensionless relative values  $(P - P_0)/P_0$  and  $(T - T_0)/T_0$  for the analysis of  $P$ - $T$ -conditions of porous fluids which are compatible for data analysis and not depth dependent. For example, the scatter plot composed of values  $(P - P_0)/P_0$  and  $(T - T_0)/T_0$  from measurements at various depths of the Kyurovdag area of the Lower Kura Depression presented in Fig. 2.9 shows the strong correlation for the area between these relative values, with a correlation coefficient of  $r = 0.77$  ( $n = 159$ ). However, there was no correlation found between values of  $(P - P_0)$  and  $(T - T_0)$ .

Interestingly, a correlation between the same parameters for a number of other oil and gas areas also yielded a strong correlation coefficient of  $r = 0.78$  ( $n = 347$ ;



**Fig. 2.9** Scatter plot of values  $(P - P_0)/P_0$  versus  $(T - T_0)/T_0$  for oil and gas fields in the Kyurovdag area of the lower Kura depression



Pilchin 1983). Similar analyses that have been conducted for such areas as the Sangachaly Sea—Duvanniy Sea—Bulla Island (Caspian Sea, Azerbaijan), Bragooni and Hayan Kort (Chechen and Ingush Republics) ( $r = 0.78$ ,  $n = 29$ ; Mekhtiev et al. 1985), Western Turkmenian Depression (Turkmenistan) ( $r = 0.87$ ,  $n = 59$ ; Mekhtiev et al. 1985) and Dowletabad area of Turkmenistan ( $r = 0.81$  for 73 fields; Mekhtiev et al. 1985) also indicate a very high correlation between  $(P - P_0)/P_0$  and  $(T - T_0)/T_0$ . Given the evidence, there is clearly a strong relationship between the relative excess of pressure and the relative excess of temperature. This is also consistent with Eqs. (2.7.4) and (2.7.5) showing functional relationship between these parameters. At the same time, it is obvious from Eq. (2.7.4) that the unloading of pressure can compromise this relationship, at least partially, which is demonstrated by the correlations.

In the case of  $\Delta V > 0$ , water contained in porous matter tends to expand, which could lead to partial unloading of pressure by moving part of the water out of the porous space. However, if such unloading cannot take place, for example when water-saturated rock is surrounded or capped by clay or a salt layer, the tendency of water to expand could in fact lead to an increase of porous pressure (Kerimov et al. 1980; Pilchin 1983) without a change in the porous volume. This thermodynamic state would be in a forced condition of equilibrium, because  $\Delta V = 0$ ,

which corresponds to Eq. (2.7.5). In such a case, the porous pressure would be maximal under conditions without external forces, since there would be no unloading of pressure.

Let us analyze the state of porous fluid under thermodynamic conditions at great depths. Any arbitrary volume  $V_0$  of a rock composed of a solid part and its porous space  $V_{p0}$  is characterized by the volume coefficient of porosity  $K_P = V_{p0}/V_0$ . The porous space is usually filled with water, in which case the solid part of the rock would have the following volume ( $V_s$ ):

$$V_s = (1 - K_P)V_0. \quad (2.7.10)$$

According to Volarovich (1978), this type of rock can be treated as a two-component system, by analyzing the solid and the fluid-filled porous parts of the rock separately. Under conditions of heating ( $T - T_0 > 0$ ), the solid part of the volume of a rock tends to expand according to the equation:

$$\Delta V_1 = \alpha_s(T - T_0)(1 - K_P)V_0, \quad (2.7.11)$$

where  $\alpha_s$  is the coefficient of volume expansion and  $T_0$  is the normal temperature of the solid part of the volume  $V_0$ .

Moreover, under pressure  $P$ , the solid part of the volume is under compression according to the following equation:

$$\Delta V_2 = \beta_s(P - P_0)(1 - K_P)V_0, \quad (2.7.12)$$

where  $\beta_s$  is the coefficient of compressibility of the solid part of the volume  $V_0$ , and  $P_0$  is the lithostatic pressure.

At the same time, any volume of rock is surrounded by other rocks that tend to expand as well and could prevent the target volume from expanding (Pilchin 1983; Pilchin and Eppelbaum 2002). In other words, any change in the volume of the solid part of a rock can only take place at the expense of the volume of the fluid-filled porous space of the volume  $V_0$ . Possible changes to the porous space can be defined by the equation:

$$\Delta V_3 = \beta_p(P - P_{AHPP})K_P V_0, \quad (2.7.13)$$

where  $\beta_p$  is the coefficient of compressibility of the porous space, after Volarovich (1978), and  $P_{AHPP}$  is the value of abnormally high porous pressure (AHPP).

By the same token, the effect of temperature and pressure on the volume of water in the porous space of a rock can be defined by the following equations:

$$\Delta V_4 = \alpha_w(T - T_{w0})K_P V_0, \quad (2.7.14)$$

$$\Delta V_5 = \beta_w(P_{AHPP} - P_{w0})K_P V_0, \quad (2.7.15)$$

where  $\alpha_w$  is the coefficient of volume expansion,  $\beta_w$  is the coefficient of compressibility of the porous water,  $T_{w0}$  is the normal temperature of water, and  $P_{w0}$  is

the hydrostatic pressure. A state of forced equilibrium  $\Delta V = 0$  for an analyzed volume of rock requires these conditions of equilibrium:

$$\Delta V_1 - \Delta V_3 = \Delta V_2, \Delta V_4 + \Delta V_3 = \Delta V_5. \quad (2.7.16)$$

This leads to a condition of equilibrium between the solid part of the volume and the porous water:

$$\Delta V_1 + \Delta V_4 = \Delta V_2 + \Delta V_5, \Delta V_4 + \Delta V_3 = \Delta V_5. \quad (2.7.17)$$

Substituting the values of  $\Delta V_1$ ,  $\Delta V_2$ ,  $\Delta V_4$  and  $\Delta V_5$  by their values from Eqs. (2.7.12–2.7.15), dividing both sides of Eq. (2.7.17) by  $V_0$  and solving the equation for  $P_{AHPP}$  produces (Mekhtiev et al. 1982):

$$P_{AHPP} = P_{w0} + \frac{\alpha_w}{\beta_w}(T - T_{w0}) + \frac{1 - K_P}{K_P} \frac{\alpha_s}{\beta_w}(T - T_0) - \frac{1 - K_P}{K_P} \frac{\beta_s}{\beta_w}(P - P_0). \quad (2.7.18)$$

Given that  $\alpha_s$  and  $\beta_s$  should be on the same order of magnitude as similar coefficients for minerals (Mekhtiev et al. 1982), their values should be around  $\alpha_s \sim 10^{-6}$ – $10^{-5}$  1/K and  $\beta_s \sim 10^{-6}$ – $10^{-5}$  1/MPa (Clark 1966). Values of similar coefficients for water are on the order of  $\alpha_w \sim 10^{-4}$ – $10^{-3}$  1/K and  $\beta_w \sim 10^{-4}$ – $10^{-3}$  1/MPa. Comparing these values and taking into consideration that the average porosity for the upper part of sedimentary cover of the Kura Depression is  $K_P = 0.25$ , the value of  $(1 - K_P)/K_P = 3$ , and that the value of lithostatic pressure is less than 2.5 times the hydrostatic pressure, it is clear that term 3 and term 4 in Eq. (2.7.18) would be negligible, yielding a result fairly similar to Eq. (2.7.5).

Another important case is when  $\Delta V < 0$ . If this condition were applied to the entire volume of a rock, it would mean that the rock is under the influence of external forces (e.g., tectonic forces), where according to Eq. (2.7.4) the pressure of this volume would even exceed the maximum pressure for situations devoid of external forces, as defined by Eq. (2.7.5). However, if  $\Delta V < 0$  were applied to the porous fluid alone, it would mean that the pores are not completely filled with fluid and have extra space available for either fluid expansion or additional fluid. Such circumstances can exist in continental areas at depths up to 0.5–1.0 km or in some oil and gas fields with abnormally low stratum pressure (ALSP) (Pilchin 1983). Since Eqs. (2.7.4) and (2.7.5) do not require any limitations or preconditions about the type of rock, mineral, initial or border conditions, they can be used for any volume and any type of matter. For example, if the porous fluid is oil, its coefficient of compressibility  $\beta_{oil}$  would be in the range of  $7$ – $140 \times 10^{-4}$  MPa $^{-1}$  (Dortman 1976), and the coefficient of volume heat expansion  $\alpha_{oil}$  in the temperature range of 273–323 K would be about  $8.54 \times 10^{-4}$  K $^{-1}$  (calculated using data in Driatskaya et al. 1971, 1972). A comparison of these values to the values of similar coefficients for water ( $\alpha_w$ ,  $\beta_w$ ) shows that the coefficient of compressibility for oil is greater on average than that of water by one order of magnitude, whereas the coefficient for volume thermal expansion remains roughly on the same order as

**Table 2.16** Values of  $K_{ap}$  of pressure in collector rocks with different degrees of saturation (Azerbaijan) (after Pilchin and Kerimov 1986)

Kind of fluid in layers	Number of wells investigated	$K_{ap}$
Gas, condensed gas	44	0.30–1.33
Oil, oil and gas	115	0.63–1.37
Water with oil and/or gas	59	1.13–1.62
Water in collectors	49	1.22–2.11
Water in clays	68	1.47–2.23

**Table 2.17** Values of  $K_{ap}$  of pressure in collector rocks with different degrees of saturation Turkmenistan ( $n = 214$ ) and Tajikistan ( $n = 217$ ) (after Pilchin and Kerimov 1986)

Kind of fluid in layers	$K_{ap}$ (Turkmenistan)	$K_{ap}$ (Tajikistan)
Gas, condensed gas	0.84–1.30	–
Oil, oil and gas	0.92–1.35	0.78–1.09
Oil	0.96–1.47	0.83–1.05
Water with oil and/or gas	1.26–1.80	1.14–2.17
Water in collectors	up to 2.00	1.20–2.41

that of water. This means that the ratio  $\alpha_{oil}/\beta_{oil}$  for oil would be on average about one order of magnitude less than that of water ( $\alpha_w/\beta_w$ ). Therefore, according to Eqs. (2.7.4) and (2.7.5) the value of the AHPP would be greater in pores filled with water than in pores filled with oil and/or gas for the same thermal conditions. This is consistent with data obtained from measurements in the oil and gas fields of Azerbaijan (see Table 2.16), and Turkmenistan and Tajikistan (see Table 2.17).

Tables 2.16 and 2.17 show that cases with  $K_{ap} < 1$  (where the pressure  $P$  is less than the hydrostatic pressure  $P_0$ ) are only present in pores of sedimentary rocks filled with either gas, oil, both gas and oil, or gas and gas condensate. At the same time,  $K_{ap}$  is maximal in water-filled pores in collector rocks and clays. Moreover,  $K_{ap}$  is the highest in clays (see Table 2.16) since they contain water bound in clay minerals which cannot be easily forced out, whereas water in collector rocks can be forced out by AHSP or AHPP. It is also clear from Tables 2.16 and 2.17 that oil and gas fields containing water do not have  $K_{ap} < 1$ . Research also shows (Pilchin 1983; Pilchin and Kerimov 1986) that the highest values of AHSP are found in fields of PreCaucasian and Middle Asia, where the thermal regime is characterized by very high temperatures and geothermal gradients ( $G$ ). By contrast, the lowest values of AHSP are found in fields characterized by low temperature values and geothermal gradients.

In numerous cases, there are signs pointing to the presence of pressures greater than the lithostatic pressure in one sector of the fields in some regions. It is obvious that in such cases AHSP played significant role in the tectonic evolution of the region. At the same time, very small values of AHSP have been found in a number of cases in active thermal fields. Such instances could be related to the fact that the values of AHSP were so high in the past that they caused an unloading of overpressure by forcing part of the porous fluid out, but subsequent cooling of

sedimentary layers in these regions led to the decline of  $K_{ap}$  under Eqs. (2.7.4) and (2.7.5), since the thermal regime in these fields was under conditions of  $\Delta T < 0$ . These facts show how important it is to analyze the thermodynamic regime in fields under maximum possible values of AHSP (or  $K_{ap}$ ), and compare these values to the lithostatic pressure to determine the change of fluid volume ( $\Delta V/V_0$ ), which characterizes both the unloading of pressure [see Eq. (2.7.4)] and the amount of fluid forced out of pores by AHSP. It should also be noted that the formation of AHSP exceeding the lithostatic pressure could lead to the emergence of fractures and the destruction of cap rock layers as a consequence of unloading the extremely high fluid pressure. For instance, such effects are well known in regions of mud volcano formation.

In the 1960s the stress–dilatancy relationship was put forward for some sedimentary rocks (Rowe 1962; Roscoe et al. 1963; Roscoe and Burland 1968), and later served to derive the dilatancy theory of earthquake prediction in the 1970s (Nur 1972, 1975; Anderson and Whitcomb 1973; Scholz et al. 1973; Cherry et al. 1975). Problems related to dilatancy models will be discussed in detail in Sect. 4.4; hence the role of porous fluid on dilatancy is only mentioned here briefly.

Dilatancy is the process by which the volume of rock increases under stress (during deformation). It is derived from the word dilation which refers to the volume expansion of brittle rock. It corresponds to an increase of volume caused by the opening of cracks, increases in porosity, and/or microfracturing of rocks. Sibson (1981) defined hydro-fracture dilatancy essentially as a low differential stress phenomenon. Aleinikov et al. (2000) proposed a new physical-mathematical conception describing the rock destruction process as a phase transition.

The significance of dilatancy in some physical applications was first pointed out by Reynolds (1885), but the stress-dilatancy theory/model was only introduced in 1962 for sands (Rowe 1962) and subsequently for soft clays (Roscoe et al. 1963). The theory would later be summarized by Roscoe and Burland (1968), Schofield and Wroth (1968), Chu et al. (2004), etc. The idea behind the stress-dilatancy theory/model is based on the experimentally discovered relationship between the main effect of dilatancy and shear strength (Rowe 1962), which thus links the stress ratio to the dilatancy rate.

It was found that at low confining pressures, dilatancy has a major influence on the shear strength of coarse-grained soils, and is largely influenced by stress level and the packing state of the soil particles (Charles 1991). Rowe (1962) showed that the stress-dilatancy relationship is more appropriate in the case of dense sand. Pender (1978) also suggested a plastic dilatancy relationship for over-consolidated clays which reveal the development of positive pore pressures in lightly and normally over-consolidated clays and negative pore pressures in heavily over-consolidated clays. This effect in clays is also discussed in Chu et al. (2004). Wan and Guo (2004) showed that under particular strain paths and fabric conditions, relatively dense sand can give way to instability or liquefaction under conditions other than isochoric. This phenomenon is consistent with laboratory experiments demonstrating that dilation (or compaction) can be controlled by modulating the amount of water flowing in or out of a sand specimen during shearing. Some

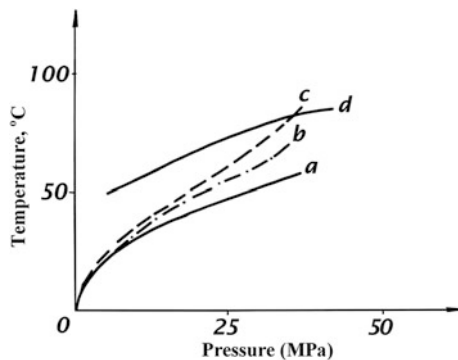


**Fig. 2.10** Changes in a unit of volume of water ( $V/V_0$ ) under different temperatures and pressures for well 558 of the Duvanniy Sea area: *a* curve of conditions for water at  $V/V_0 = 1.00$ ; *b* curve of conditions in the well with unloading of layer from excess water ( $V_2/V_0$ ); *c* curve of conditions in the well without unloading of layer from excess water ( $V_1/V_0$ ); *d* curve of condition of water with  $V/V_0 = 1.01$

studies help relate the plastic dilatancy ratio to the development of pore pressures in clay soils (Chu et al. 2004). Authors have also noted the importance of effective pressure, which is defined as the total pressure minus the porous pressure, for saturated and dry rocks (e.g., Scholz et al. 1973) in analyzing dilatancy.

From all of the above, it is clear that dilatancy is strongly related to the porosity of sedimentary rocks and porous pressure. It is also evident that Eq. (2.7.4) can be used to determine or estimate the relative volume change ( $\Delta V/V_0$ ) that can be used to characterize dilatancy in sedimentary rocks and rock layers. From this point of view, it also seems important to analyze the variable volume ( $\Delta V/V_0$ ) in relation to maximal porous pressure for sedimentary layers in different regions with varying thermodynamic regimes.

Equation (2.7.4) can be used to calculate the relative change of volume ( $\Delta V/V_0$ ) of porous fluid.

In fact, solving Eq. (2.7.4) for  $\Delta V/V_0$  yields:

$$\frac{\Delta V}{V_0} = \alpha(T - T_0) - \beta(P - P_0). \quad (2.7.19)$$

It is clear from Eq. (2.7.19) that it can be used to determine the amount of water forced out by AHSP/AHPP in a case where  $(T - T_0) > 0$ , as well as the relative reduction in fluid volume (and/or amount of porous volume available for additional fluid) in a case where (ALSP/ALPP) of  $(T - T_0) < 0$ . Thus if  $(T - T_0) > 0$ , the amount of fluid (usually water) forced out of pores by AHSP/AHPP is defined as the difference between the values  $V_1/V_0$  and  $V_2/V_0$  shown in Fig. 2.6 for cases where there is no fluid unloading ( $\Delta V = 0$  and  $P_{AHPP}$  is maximal without unloading), and real volume conditions (with the measured value of  $P_{AHPP}$ ), respectively. For example, such a determination for well 558 of the Duvanniy Sea area is presented in Fig. 2.10.

The relative change of the volume of water ( $\Delta V_{12}$ ) for each pair of  $P$  and  $T$  values can be determined from the equation:

$$\frac{V_{12}}{V_0} = \frac{V_1}{V_0} - \frac{V_2}{V_0}. \quad (2.7.20)$$

It should be taken into account that changes in the volume of porous water do not imply changes in the porous volume, since even though in most cases part of the water would be forced out by the AHSP/AHPP, the remaining water would fill the porous volume. However, the density of the remaining water would be different from that of the porous water prior to unloading. If under certain  $P$ - $T$ -conditions the initial volume of water  $V_0$  has a density  $\sigma_0$ , the average change in density with variable volume  $V$  would be:

$$\Delta\sigma = K_P \frac{V_0 - V}{V} \sigma_0. \quad (2.7.21)$$

Depending on the thermodynamic conditions, a volume of water could decrease, leading to an increase in its density and a positive gravity effect. Conversely, an increase in volume is also possible, which would lead to decreased density in the case of unloading of part of the water from the porous volume. Using geothermal data and Figs. 2.6 and 2.10, the change in a unit of volume ( $V/V_0$ ) and the corresponding change in density ( $\Delta\sigma$ ) for each 1 km interval to a depth of 4 km, and subsequently the average values of  $V/V_0$  and  $\Delta\sigma$  for the upper 4 km layer were calculated for some regions of the Kura Depression (Azerbaijan) and adjacent areas of the Caspian Sea (see Table 2.18). Data on variable density were also used to determine the gravity effect of such a change in density for selected oil and gas fields, as also presented in Table 2.18. A maximum depth of 4 km for the estimates was selected for the following reasons: (1) a significant distance from the surface layers below a depth of 4 km would have a very small effect on the gravity field; (2) at depths of over 4 km, porosity can be much smaller, and likewise produce a much smaller effect; (3) if the upper 4 km layer showed some significant gravity effect, including lower layers could only serve to increase this effect, whereas the purpose of these estimates is first and foremost to verify the presence of a gravity effect.

It can be seen from Table 2.18 that the values of both  $V/V_0$  and  $\Delta\sigma$  are very small, but they create quite a significant gravity effect  $\Delta g$ , on the same order of magnitude as the gravity effect caused by oil and gas fields, which enables the use of high definition gravity for prospecting for oil and gas fields. Note that the value of the density change of water is negative for all these areas, which points to the unloading of some water from the porous volume. However, this effect may simply be typical of the region, and not useful for further interpretation. To verify this possibility, the gravity effect caused by variable density under thermodynamic conditions was estimated for different parts (crest and slope) of anticline structures on the Muradkhanly and Kyursangya areas (Azerbaijan). The results of these estimates are presented in Table 2.19.

**Table 2.18** Average changes in the density of water, and gravity effect caused by these changes under the thermodynamic conditions of some oil and gas areas of the Kura depression and adjacent areas of the Caspian sea

Area	Average change of unit of volume of water ( $V/V_0$ )	Average change of density of water [ $\Delta\sigma$ (kg/m <sup>3</sup> )]	Value of gravity effect ( $\Delta g$ in mGal)
Borsunly	1.030	−6.1	−1.00
Sovetlyar	1.023	−4.7	−0.73
Zardob	1.017	−3.5	−0.54
Muradkhanly	1.022	−4.5	−0.69
Sor-Sor	1.012	−2.7	−0.38
Dzharly	1.011	−2.6	−0.38
Padar	1.010	−2.5	−0.37
Kalamadin	1.006	−1.5	−0.31
Kyurovdag	1.009	−2.3	−0.36
Karabagly	1.002	−0.6	−0.13
Kyursangya	1.009	−2.3	−0.36
Sangachali Sea	1.016	−3.5	−0.54
Garadag	1.016	−3.5	−0.54
Duvanniy Sea, Bulla island	1.016	−3.5	−0.54

**Table 2.19** Estimates of the gravity effect caused by changes in the density of porous water for the Muradkhanly and Kyursangya areas

Area	Average change of unit of volume of water ( $V/V_0$ )	Average change of density of water [ $\Delta\sigma$ (kg/m <sup>3</sup> )]	Value of gravity effect ( $\Delta g$ in mGal)
<i>Muradkhanly</i>			
Crest	1.023	−4.7	−0.72
NE Slope	1.015	−3.1	−0.49
<i>Kyursangya</i>			
Crest	1.013	−3.0	−0.49
Slope	1.005	−1.3	−0.20

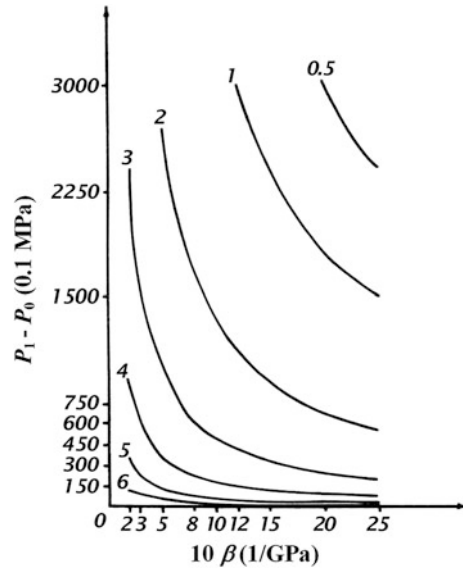
Table 2.19 indicates that the gravity effect for these areas is considerable and the difference between its effect for the crest and the slope of these anticline structures is −0.23 mGal for the Muradkhanly area and −0.29 mGal for the Kyursangya area. These values are significant and can be measured with gravimeters. Moreover, these values are on the order of the gravity effect formed by oil and gas fields, and consequently in some cases anomalies in the gravity field caused by the reduction of density of water under thermodynamic conditions could be mistaken for ones caused by oil and gas fields.

From Eq. (2.7.5), accepting  $P_1$  as the maximal possible pressure defined as the pressure without unloading (see above),  $P_1$  can be defined as:

$$P_1 = P_0 + \frac{\alpha}{\beta}(T - T_0). \quad (2.7.22)$$



**Fig. 2.11** Chart for determining the change in volume of water [in  $-\lg(\Delta V/V_0)$ ]



Equation (2.7.22) can be written as:

$$\beta(P_1 - P_0) = \alpha(T - T_0). \quad (2.7.23)$$

Substituting  $\alpha(T - T_0)$  from Eq. (2.7.23) into Eq. (2.7.19) and solving it for  $P$  gives:

$$P = P_1 - \frac{1}{\beta} \frac{\Delta V}{V_0}. \quad (2.7.24)$$

Finally, Eq. (2.7.24) can be presented as (Mekhtiev et al. 1982):

$$\frac{\Delta V}{V_0} = \beta(P_1 - P). \quad (2.7.25)$$

Equation (2.7.25) was used for compiling Fig. 2.11, which can be used to determine the  $\Delta V/V_0$  of water for different  $P$ - $T$ -conditions (Mekhtiev et al. 1982).

In order to determine the value of total possible unloading of porous volume from water caused by  $P$ - $T$ -conditions in Eq. (2.7.24), note that  $P$  should be replaced by  $P_0$ . Determining the  $\Delta V/V_0$  for both  $P$  and  $P_0$  can serve to estimate the excess fluid (water) contained in porous volumes under the given  $P$ - $T$ -conditions. It can also be used to estimate the quantity (reserves) of fluid/water in a layer.

Equation (2.7.24) was used to analyze the amount of unloading of layers in some oil and gas areas of West and East PreCaucasian. Research shows that in Azerbaijan, the highest values of unloading of porous volume in layers are found in areas of Middle Kura Depression (Pilchin 1983). Estimates made for 23 wells of Muradkhanly area returned a value of water volume change of  $\Delta V/V_0 = 0.035$ – $0.070$  or 3.5–7.0 % of the total porous fluid. Significantly lower  $\Delta V/V_0$  values were

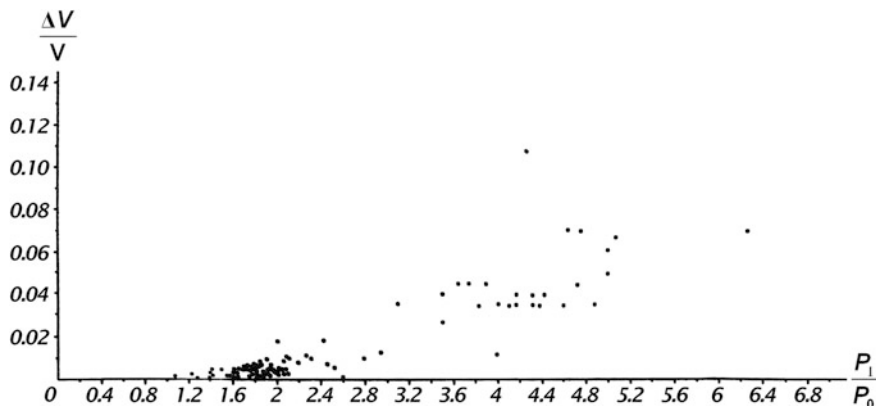


**Fig. 2.12** Dependence of values of relative change in the volume  $\Delta V/V_0$  on the maximal value of  $K_{aP} = P_1/P_0$  for oil and gas fields of Azerbaijan

obtained for areas of the Lower Kura Depression: for 51 wells in Kyurovdag area  $\Delta V/V_0 = 0.005\text{--}0.027$  (or 0.5–2.7 %); 21 wells of Kalmas area  $\Delta V/V_0 = 0.003\text{--}0.011$  (or 0.3–1.1 %); 7 wells of Mishovdag area  $\Delta V/V_0 = 0.0005\text{--}0.0120$  (or 0.05–1.2 %). Very low values of  $\Delta V/V_0$  were found for areas of the Caspian Sea: for well 550 in the Sangachaly Sea area  $\Delta V/V_0 = 0.0005\text{--}0.0050$  (or 0.05–0.5 %); well 558 in the Duvanniy Sea area  $\Delta V/V_0 = 0.0023$  (or 0.23 %). Similar estimates of the unloading of porous volume from an excess of fluid for the PreCaucasian (Mekhtiev et al. 1982) yielded the following values:  $\Delta V/V_0 = 0.001\text{--}0.070$  (or 0.1–7.0 %) for 21 wells of Hayan Kort area and  $\Delta V/V_0 = 0.045\text{--}0.086$  (or 4.5–8.6 %) for the Braguni area. As a whole, the Western PreCaucasian (30 wells) and Eastern PreCaucasian (55 wells) values of  $\Delta V/V_0$  were 0.022–0.091 (or 2.2–9.1 %) and 0.018–0.177 (or 1.8–17.7 %), respectively. These values indicate that high temperatures in the layers of the PreCaucasian force out up to 17.7 % of their normal volume from their porous space. For a better understanding of the influences of the variable volume of fluid  $\Delta V/V_0$ , the relationships between values of  $\Delta V/V_0$  and  $P_1/P_0$  are presented in Figs. 2.12 and 2.13 for oil and gas fields in Azerbaijan and the PreCaucasian, respectively. From the definition of  $P_1$  (see above), it is clear that the value of  $P_1/P_0$  represents the maximum possible value of  $K_{aP}$  in the high temperature regime in a region.

Figures 2.12 and 2.13 show that for both regions increased values of  $K_{aP} = P_1/P_0$  go hand in hand with increased  $\Delta V/V_0$  values.

Interestingly, for the 23 wells of the Muradkhanly area  $P_1/P_0 = 3.09\text{--}6.25$ , the lithostatic pressure  $P_{lit}$  at the same depths is only  $\sim 2.5$  times greater than the hydrostatic pressure  $P_0$  ( $P_{lit}/P_0 = 2.5$ ). This means that in the oil and gas fields of the Muradkhanly area, the value of  $P_{AHSP}$  could have been greater than the lithostatic pressure  $P_{lit}$ . Such a situation could have led to the formation of the types of cracks and dilatancy discussed above. This is consistent with results of studies by Sibson (1981) reporting arrays of parallel extension fractures and veins

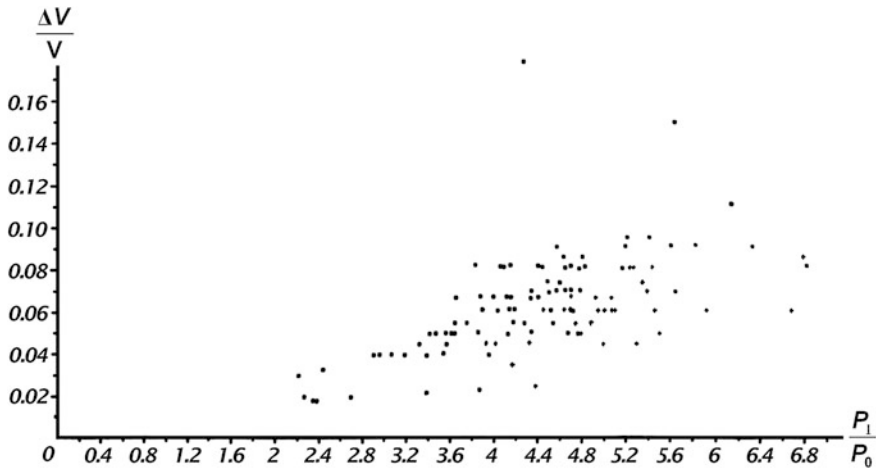


**Fig. 2.13** Dependence of the value of the relative change in volume  $\Delta V/V_0$  on the maximal value of  $K_{aP} = P_1/P_0$  for oil and gas fields of the PreCaucasian

associated with exhumed faults that appear to be the product of repeated hydrofracturing under a shared stress regime, which can only occur in association with thrusts when fluid pressures exceed the lithostatic load. Moreover, it is clear that the highest possible value of AHSP/AHPP could have been 2.5 times greater than the lithostatic pressure. However, such high pressures could not have actually been collected prior to the start of its unloading, since porous pressure primarily generates tensile stress, whereas the tensile stress limits of any rocks and especially sedimentary rocks is very low (e.g. Clark 1966). The presence of significant pressure unloading is also proven by data from other authors (e.g., Magara 1978). The value of AHSP/AHPP would increase gradually and likewise be gradually unloaded. In other words, even though the maximal possible AHSP/AHPP could be very high it would unload throughout the entire period of evolution of the layer.

In the oil and gas fields of the Lower Kura Depression areas (Pilchin 1983), the maximum possible AHSP/AHPP is much lower, and the value of  $P_1/P_0$  is 1.18–3.50 (for 51 wells of the Kyurovdag area); 1.42–4.00 (for 8 wells of the Mishovdag area); 1.42–2.94 (for 21 wells of Kalmas area). For well 550 in the Sangachaly Sea area, the value of  $P_1/P_0$  is in the range of 1.55–2.11; i.e., in layers of the Sangachaly Sea area (Azerbaijan) AHSP/AHPP was never greater than the lithostatic pressure  $P_{Lit}$ . For areas of the PreCaucasian, the values of possible maximum AHSP/AHPP are very high and the value of  $P_1/P_0$  is 2.26–6.80 for 116 readings, and values of  $P_1/P_0 < 3.0$  have only been determined for 9 points. For areas of Turkmenistan (Kerimov and Pilchin 1986b), these values are Western Turkmenistan  $\Delta V/V_0 = 0.0020$ – $0.0203$ ,  $P_1/P_0 = 1.69$ – $2.64$  (for 24 wells); Central Turkmenistan  $\Delta V/V_0 = 0.0020$ – $0.0263$ ,  $P_1/P_0 = 3.68$ – $7.79$  (for 68 wells); and Eastern Turkmenistan  $\Delta V/V_0 = 0.0129$ – $0.0610$ ,  $P_1/P_0 = 3.57$ – $6.53$  (for 84 wells).

It should be stated that in all cases, the highest  $P_1/P_0$  ratio and the relative change of volume  $\Delta V/V_0$  are regulated by the thermal regime in the sedimentary layers. For example, in the Kura Depression the geothermal gradient is about 39–43 K/km in its westernmost part, drops to 20–30 K/km in the central part of the Middle Kura Depression, and further declines to 18–20 K/km in the eastern part of the Lower Kura Depression (Mekhtiev et al. 1985; Kerimov and Pilchin 1986a). In depression zones of the Northern Caucasus (including the Pre-Caucasian), the geothermal gradient is in the range of 25–60 K/km, and in some isolated cases even greater (Mekhtiev et al. 1985; Kerimov and Pilchin 1986a). The geothermal gradients for areas of Western Turkmenistan are within the range of 21–28 K/km, increasing in areas of the Central Turkmenistan and reaching 40–60 K/km, and then declining to 31–39 K/km in areas of Eastern Turkmenistan (Mekhtiev et al. 1985; Kerimov and Pilchin 1986a).

Thus overall, dilatancy indeed exists and has been found to take place in a wide range of regions. If the dilatancy effect were not present, the obtained pressure values in all cases would be equal to the maximum possible value of  $P_1$ . However, in fact, all these pressures were much lower than the maximum of AHSP/AHPP. Thus, unloading of pressure took place in all the cases mentioned above, and according to Eq. (2.7.4) the value of the change in volume  $\Delta V$  was never zero. It is also clear that if at very shallow depths (up to 500–1,000 m, at which the zone of AHSP/AHPP usually begins) the pores were permeable all the way through to the surface, it would allow the unloading fluid flow to reach the surface without forming cracks and fractures. However, such a situation would not be possible for fluid within layers capped by impermeable layers (e.g., clay or salt layers). At the same time, most of the data used for the above analysis were taken from measurement values of temperatures and pressures in layers containing oil and gas fields, which are most certainly capped by clay layers in Azerbaijan, the Caspian Sea, Western Turkmenistan and the PreCaucasian, and capped by salt layers in Eastern Turkmenistan and Uzbekistan. Additionally, it can be seen from Tables (2.16) and (2.17) that in all cases, pressures in fields, including fields filled with water, are much lower than the maximum possible pressure under the present thermal regime. Data from other regions of Russia, Ukraine, Kazakhstan and Uzbekistan also support this trend (Table 2.20).

Such values (Table 2.20) are only possible if dilatancy took place, since in layers below the cap layer an increase in volume is possible only by forming cracks and fractures. Since the average density of the upper sedimentary layers is about 2,350 kg/m<sup>3</sup>, it follows that the lithostatic pressure ( $P_{lit}$ ) in such layers should be about 2.35 times greater than the hydrostatic pressure ( $P_0$ ), and  $P_{lit}/P_0 = 2.35$ . At the same time, it was shown above that the maximum values of  $K_{ap} = P_1/P_0$  can be as high as 7.79 for Central Turkmenistan. This means that the total possible maximum values of AHSP/AHPP ( $P_1$ ) can be greater than the lithostatic pressure ( $P_1/P_{lit}$ ) by up to 2.7 times for the Middle Kura Depression, 1.7 times for the Lower Kura Depression, 2.9 times for the PreCaucasian, 1.1 times for the Western Turkmenistan, 3.3 times for Central Turkmenistan and 2.8 times for Eastern Turkmenistan. Naturally, at such shallow depths the lithostatic pressure

**Table 2.20** Values of  $K_{ap}$  of pressure in fields with different kinds of fluid saturation for some areas of Russia, the Ukraine, Kazakhstan, and Uzbekistan

Region	Kind of porous fluid					No. of tests
	Gas, condensed gas	Gas, oil	Oil	Hydrocarbons and water	Water	
Permian province	–	0.88–1.14	0.9–1.13	–	–	52
Bashkortystan	–	0.55–1.03	0.74–1.35	–	–	161
Orenburg province	0.84	0.72–1.19	1.03–1.11	–	–	30
Kuybishev province	–	0.79–1.14	0.81–1.19	–	–	65
Komi republic	–	0.64–1.04	0.75–1.12	–	–	29
Stavropol province	–	0.96–1.22	0.98–1.19	–	–	38
Krasnodar province	–	0.51–1.32	0.47–1.45	–	–	60
Sakhalin Island	–	0.84–1.16	0.64–1.17	–	–	118
Napsko-Botuobinskiy	0.71–1.23	–	0.72–1.43	–	–	59
Dnieper-Donets	0.95–1.26	0.76–1.13	1.00–1.16	–	up to 1.8	106
PreCarpathian	0.81–1.49	0.44–1.12	0.67–1.52	1.31–1.61	to 2.02	67
Crimea	0.50–1.19	0.75–1.02	1.03–1.52	1.02–1.88	to 2.19	58
Precaspian	–	–	0.53–1.39	1.25–1.55	–	163
	–	1.00–1.35	–	1.21–1.46	–	17
South-Mangyshlak	1.10–1.20	0.55–1.32	0.56–1.40	1.23–1.77	–	52
Fergana						

would be unable to maintain such enormous pressures. This also means that dilatancy was in most cases caused by an increase of AHSP/AHPP.

The highest value of  $\Delta V/V_0$  taken from the above results is 17.7 %. Since this is the change in the fluid part of the volume alone, for sedimentary rock with a porosity of  $\sim 25$  % it would yield a maximum change of the rock volume of about 4.425 %. We can then conclude that the value of dilatancy in all cases was no more than 4.425 %. At the same time, as was shown earlier, the maximal possible pressure cannot be accumulated completely until the start of its unloading, and it would continue unloading bit by bit as it was increasing. Given that this volume was growing a little at a time over millions and tens of millions of years (e.g., the Muradkhanly oil and gas field are within Mesozoic layers in Central Azerbaijan), it is obviously very difficult to measure this effect in nature. Pinpointing the dilatancy effect in depressional regions through seismological investigation is hence a very complicated task.

It was mentioned above that in the case of regional tectonic activity, the value of  $\Delta V/V_0$  may be less than zero, indicating an additional pressure increase beyond its maximum possible value as a result of the thermal regime. Such cases were reported by Kerimov and Pilchin (1986b) based on water density values under layer conditions for wells 666 and 680 (at depths of 1.51 and 4.45 km, respectively) of the Starogroznenskiy area and well 503 (depth 3.35 km) of the Orliniy area of the Tersko-Sunzhensk Depression, for all of which the value of the ratio  $\Delta\sigma/\sigma > 0$ . This feature, in addition to the positive value of compressibility ( $\beta > 0$ )

in Eq. (2.7.8) points to an additional increase in pressure above and beyond the value caused solely by the thermal regime. This means that in these cases, tectonic stresses in sedimentary layers contributed significantly to the abnormal pressure values.

Kerimov and Pilchin (1986b) showed that analysis of the geothermal regime of layers at great depths can be used to identify conditions related to the presence of oil and gas in different layers. Theoretically, this problem can be solved as follows. Assume that there is a two-component field containing oil and water, characterized by a field pressure  $P_1$ , temperature  $T_1$  and coefficients of expansion and compressibility for oil  $\alpha_o$ ,  $\beta_o$  and water  $\alpha_w$ ,  $\beta_w$ , respectively. If the thermodynamic conditions within the field were to somehow change to pressure  $P_2$  and temperature  $T_2$ , there would be a re-distribution of the initial volumes of oil ( $V_{o0}$ ) and water ( $V_{w0}$ ). The relative change in volumes of oil and water respectively, would be characterized by the state equations:

$$\frac{\Delta V_o}{V_{o0}} = \alpha_o(T_2 - T_1) - \beta_o(P_2 - P_1). \quad (2.7.26)$$

$$\frac{\Delta V_w}{V_{w0}} = \alpha_w(T_2 - T_1) - \beta_w(P_2 - P_1). \quad (2.7.27)$$

Under these changes to the components, the initial volumes in the field value of the total volume of both fluids would be constant:

$$V_{o0} + V_{w0} = \text{const.} \quad (2.7.28)$$

Thus, changes to one component of the fluid mixture in the field could only take place at the expense of a volume change in the other component:

$$\Delta V_o = -\Delta V_w. \quad (2.7.29)$$

Dividing Eq. (2.7.27) by Eq. (2.7.26) and taking into account the condition in Eq. (2.7.29), one gets:

$$\frac{V_{o0}}{V_{w0}} = -\frac{\alpha_w(T_2 - T_1) - \beta_w(P_2 - P_1)}{\alpha_o(T_2 - T_1) - \beta_o(P_2 - P_1)}. \quad (2.7.30)$$

Let us term the value of the ratio  $V_{o0}/V_{w0}$  the coefficient of relative oil content  $\mu$ :

$$\mu = \frac{V_{o0}}{V_{w0}}. \quad (2.7.31)$$

It is clear from Eq. (2.7.31) that for  $\mu = 1$ , the initial volumes of oil and water are equal; for  $\mu > 1$  oil has a higher volume than water in the field. In such a case,  $K_o > K_w$ . In particular, in a case where  $\mu \rightarrow \infty$ , there would be very little water content in that field. At the same time, for  $\mu < 1$  the volume of water would be

greater than that of oil, and if  $\mu \rightarrow 0$  the field would contain very little oil. Thus, by using the coefficient of the relative oil content, it is also possible to estimate the coefficient of the oil saturation of rocks ( $K_o$ ) from:

$$K_o = \frac{1}{1 + \frac{1}{\mu}}. \quad (2.7.32)$$

## 2.8 Density of Fluids in the Early Earth Atmosphere

As it was discussed in Sect. 1.1, various sources generated energy during the Earth's formation and evolution, the most significant of which were planetary accretion, planetary differentiation, bombardment by huge astronomic objects (planetesimals, asteroids, etc.), and the radioactive decay of short-lived and long-lived radioisotopes (Lubimova 1968a; Pollack 1997). Estimates of the combined energy produced by these processes, even disregarding the Earth's possible collision with a Mars-sized body, show that the energy was sufficient to melt the entire planet during its accretion (Lubimova 1968a, b; Pollack 1997; Valley et al. 2002).

It is generally accepted that for some period in its early evolution, the Earth was entirely covered by a magma-ocean (Abe 1997; Li and Agee 1996; Pollack 1997; Labrosse et al. 2007; Righter and Drake 1997b; Sleep et al. 2001; Solomatov 2000; Valley et al. 2002; Pilchin and Eppelbaum 2006, 2009), which was between several hundred (Walter and Trønnes 2004) up to about 1,000 km deep (Li and Agee 1996; Labrosse et al. 2007). Some scientists believe that this magma-ocean could only have existed for about 1–10 million years (Spohn and Schubert 1991), while others argue that it could have remained for 100–200 million years (Abe 1997; Pollack 1997), and could have persisted for even a few hundred million years in the case of a thick early atmosphere (Abe 1997; Solomatov 2000). This type of magma-ocean was also present at one time on other terrestrial planets and the Moon (Matsui and Abe 1986; McSween 1993).

The content and composition of the early Earth's atmosphere above this magma-ocean would have been determined by the stability conditions of the chemical compounds existing in the solar nebula and the developing planetesimals, asteroids and other cosmic objects. Previous studies have shown that the early Earth's atmosphere was rich in carbon dioxide and water vapor (Table 2.21).

Numerous compounds (chlorides, hydrides, oxides, sulfides, sulfates, sulfites, nitrates, etc.) decompose at temperatures lower than those of the magma-ocean (Lide 2005; Speight 2005; Pilchin and Eppelbaum 2006). For example,  $K_2O$  decomposes at 623 K (Lide 2005),  $Na_2O$  at 1,445 K (Lide 2005),  $Ni_2O_3$  at 873 K (Lide 2005),  $NaH$  at 698 K (Lide 2005), etc. This means that some compounds and even pure elements would have been in the atmosphere over the magma-ocean,

**Table 2.21** Estimates of the partial pressure of carbon dioxide and water vapor in the early Earth's atmosphere

Atmosphere Component	Age	Partial pressure (MPa)	References
Carbon dioxide, CO <sub>2</sub>	Hadean	1	Morse and Mackenzie (1998)
	After end of accretion	A few MPa	Abe (1993)
	First several hundred Ma	1–2	Kasting and Ackerman (1986)
	Early earth atmosphere	10–100	Sukumaran (2001)
	Early earth atmosphere	1	Walker (1985)
	Proto-atmosphere	10	Liu (2004)
	Early earth atmosphere	Up to 4.35	Pilchin (2011)
Water vapor, H <sub>2</sub> O	Hadean	All water was vaporized	Pollack (1997)
	Right after accretion	20–30	Abe (1993)
	Early earth atmosphere	10–30	Zahnle et al. (1988)
	Early earth atmosphere	27	Zahnle et al. (1988)
	Proto-atmosphere	56	Liu (2004)
	Early earth atmosphere	~ 30	Genda and Ikoma (2008)
	Early earth atmosphere	~ 26	Pilchin and Eppelbaum (2009)

since they have relatively low boiling points of 1,032 K for K (potassium), 1,156 K for Na, 717.7 K for S, and 1,180 K for Zn (Lide 2005; Speight 2005).

As was discussed earlier, even though other compounds have greater temperatures of decomposition, they could still have sunk in the magma-ocean to hotter depths where they would have decomposed and released volatiles, which would once again have eventually ended up in the atmosphere. All of this means that the atmosphere above the magma-ocean was rich in all the typical atmospheric gases, volcanic gases, as well as numerous other compounds which would have existed in a gaseous state at those temperatures.

Observing gases released during different magmatic activities reveals (Hall 1995; Stoiber 1995; Textor et al. 2004) that H<sub>2</sub>O, SO<sub>2</sub> and CO<sub>2</sub> are by far the chief components of any volcanic process. This makes an examination of the conditions of stability of carbon and sulfur compounds, as well as water, a key to any investigation of the composition of the early atmosphere.

Analyses of published experimental data show (Pilchin and Eppelbaum 2006) that none of the main carbonate rocks (limestone, dolomite, calcite, siderite, magnesite, K<sub>2</sub>CO<sub>3</sub>, Na<sub>2</sub>CO<sub>3</sub>, etc.) are stable at temperatures above 1,173–1,193 K, and that the temperatures for their stability are generally a great deal lower (Lide 2005; Speight 2005; Pilchin and Eppelbaum 2009). This means that at the time of the magma-ocean, none of these carbonates would have survived and must have decomposed, releasing CO<sub>2</sub>.

A similar analysis of publications on the conditions of pyrite stability shows that the maximum temperature at which it is stable is about 1,016 K, and is usually



much lower (Lide 2005; Pilchin and Eppelbaum 2006; Speight 2005). Experimental data also show that pyrrhotite is unstable above  $\sim 1,463$  K, and pyrite is stable below  $\sim 873$  K (Lide 2005; Speight 2005). Furthermore, pyrite decomposes at temperatures of 743 K in a  $\text{CO}_2$  atmosphere (Golden et al. 2004). As such, since neither pyrite nor pyrrhotite could have been stable within the magma-ocean, elemental sulfur would have been released into the atmosphere after their decomposition. It can be seen from data presented in (Lide 2005; Speight 2005) that a number of sulfides, sulfites and sulfates would likewise have been unstable under such conditions. For example, iron(III) sulfate decomposes at a temperature of  $\sim 1,451$  K (Speight 2005) and nickel sulfate decomposes at a temperature of  $\sim 1,113$  K (Lide 2005).

Analysis of the composition of magmatic gases collected from basaltic lavas during eruptions (Hall 1995) shows that their main components are  $\text{H}_2\text{O}$ ,  $\text{SO}_2$  and  $\text{CO}_2$ , and that the average content of  $\text{SO}_2$  is second by volume to water and first by weight. Textor et al. (2004) further indicated that the dominant sulfur component of volcanic gases is sulfur dioxide ( $\text{SO}_2$ ). Furthermore, given the immense temperatures, no liquid water could have existed on the Earth's surface at the time of the magma-ocean, and it all would have been in vaporous form in the atmosphere.

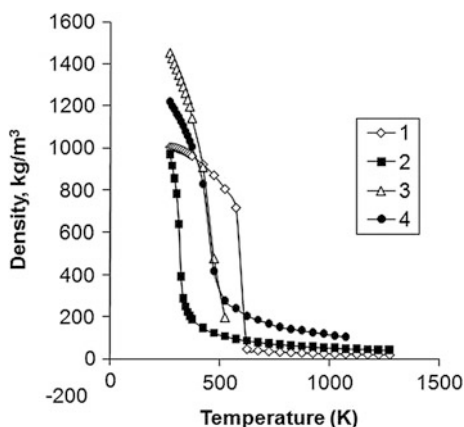
All of the above shows that during the formation and evolution of the magma-ocean there would have been a very dense and thick atmosphere. This corresponds to other studies showing that the primitive atmosphere and ocean appear to have been formed from gases arising from the magma-ocean (Drake 2000).

Estimates of the pressure generated by such an atmosphere indicate a minimum value of  $\sim 35$  MPa (Pilchin and Eppelbaum 2006). This estimate represents the absolute minimal possible atmospheric pressure, because the amount of water used for the calculations was that of the current day ocean and subsurface underground content. For example, the partial pressure of water alone calculated using estimates of its content in the biosphere, hydrosphere and crust presented in (Holland 1984) is  $\sim 39$  MPa. Estimates by Zhang and Zindler (1993) show that the amount of carbon dioxide currently bound in carbonate rocks is sufficient to generate an additional partial pressure of  $\sim 21.5$  MPa. The estimated partial pressure of carbon oxides within the early Earth's atmosphere to determine the abundance of carbon presently within the crust alone indicate 2.99 MPa for carbon as  $\text{CO}$ , and 4.35 MPa for carbon as  $\text{CO}_2$  (Pilchin 2011). Similar estimates of the partial pressure within the early Earth's atmosphere from such elements as F, Cl, and S, as well as their compounds using the abundance values of these elements within the present crust alone (Pilchin 2011) indicate minimal values of 4.35 MPa for elemental  $\text{F}_2$ , 2.72 MPa for elemental  $\text{Cl}_2$ , 2.72 MPa for elemental  $\text{S}^0$ , and 5.44 MPa for sulfur as  $\text{SO}_2$ .

Some studies have concluded that the water content on Earth at the time could have been equal to about 5–6 current Earth oceans, and even up to 50 Earth oceans [see review in Drake (2005)]. Stimpfl et al. (2004) and Drake (2005) calculated

**Table 2.22** Critical properties of some fluids after (Rau et al. 1973; Reid et al. 1987; Lide 2005; Speight 2005; Yaws 2001, 2008)

Fluid	Temperature (K)	Pressure (MPa)	Density (kg/m <sup>3</sup> )
Carbon dioxide, CO <sub>2</sub>	304.1	7.38	468
Water, H <sub>2</sub> O	647.3	22.12	322
Methane, CH <sub>4</sub>	190.4	4.60	162
Hydrogen sulfide, H <sub>2</sub> S	373.2	8.94	349
Sulfur dioxide, SO <sub>2</sub>	430.7	7.88	525
Sulfur trioxide, SO <sub>3</sub>	491.1	8.20	633
Oxygen, O <sub>2</sub>	154.6	5.04	436
Carbon monoxide, CO	132.9	3.50	1,465
Carbon disulfide, CS <sub>2</sub>	552.0	7.90	476
Chlorine dioxide, ClO <sub>2</sub>	465.0	8.61	690
Sulfuric acid, H <sub>2</sub> SO <sub>4</sub>	925.0	6.40	552
Sulfur monochloride, S <sub>2</sub> Cl <sub>2</sub>	659.4	6.28	554
Trisulfur dichloride, S <sub>3</sub> Cl <sub>2</sub>	489.7	3.58	560
Carbonyl sulfide, COS	378.8	6.35	445
Chlorine, Cl <sub>2</sub>	417.0	7.71	573
Sulfur, S <sub>n</sub>	1,313.0	18.2	563

**Fig. 2.14** Changes in the density of H<sub>2</sub>O, CO<sub>2</sub>, and SO<sub>2</sub> with increases in temperature under pressure of 10 MPa: (1) H<sub>2</sub>O, (2) CO<sub>2</sub>, (3) SO<sub>2</sub> from experimental data (Ihmels et al. 2003), (4) SO<sub>2</sub> calculated using thermodynamic methods for fluids

that the amount of water adsorbed in the Earth during accretion could have been as much as 1–3 Earth oceans. Needless to say, this would have dramatically increased the atmospheric pressure. At the same time, both the temperature and pressure within the Earth's atmosphere are variable with altitude. This means that at different altitudes within the early Earth's atmosphere there would have been different values of pressure, temperature, and therefore density. It is also important to note that the key components of the early Earth's atmosphere (H<sub>2</sub>O, SO<sub>2</sub>, CO<sub>2</sub>, etc.) would have been under supercritical conditions (Table 2.22).

**Fig. 2.15** Changes in the density of H<sub>2</sub>O, CO<sub>2</sub>, and SO<sub>2</sub> with increases in temperature under pressure of 25 MPa: (1) H<sub>2</sub>O, (2) CO<sub>2</sub>, (3) SO<sub>2</sub> from experimental data (Ihmels et al. 2003), (4) SO<sub>2</sub> calculated using thermodynamic methods for fluids

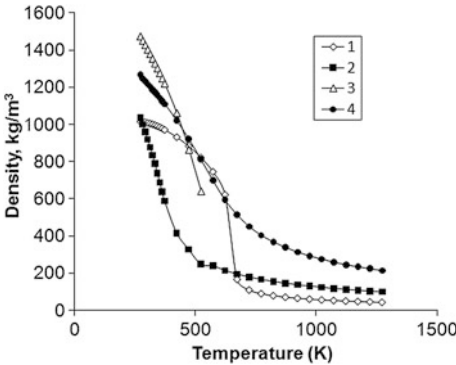


**Fig. 2.16** Changes in the density of H<sub>2</sub>O, CO<sub>2</sub>, and SO<sub>2</sub> with increases in temperature under pressure of 35 MPa: (1) H<sub>2</sub>O, (2) CO<sub>2</sub>, (3) SO<sub>2</sub> from experimental data (Ihmels et al. 2003), (4) SO<sub>2</sub> calculated using thermodynamic methods for fluids

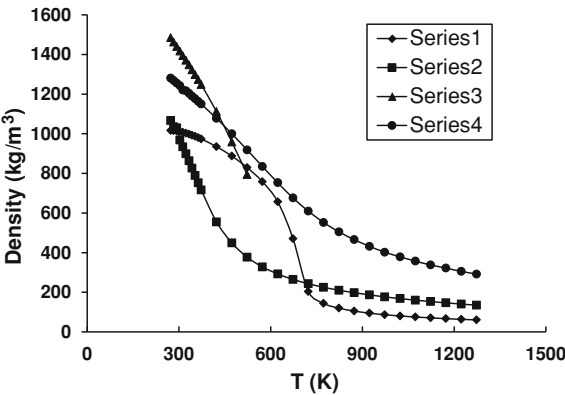


**Table 2.23** Temperature range within which the density of water is greater or about the same as the densities of SO<sub>2</sub>, CO and CO<sub>2</sub> at different pressures (adapted from Pilchin 2011)

Atmosphere component	Temperature range (in K) at pressure				
	10 MPa	25 MPa	35 MPa	50 MPa	100 MPa
SO <sub>2</sub> , calculated	~400–600	~500–600	None <sup>a</sup>	None <sup>a</sup>	None <sup>a</sup>
SO <sub>2</sub> , from experimental data	~400–?	~450–?	~500–550	–	–
CO <sub>2</sub>	<~600	~280–650	~300–700	~315–760	360–780
Co	–	–	~415–630	–	–

<sup>a</sup> Below this pressure the densities of SO<sub>2</sub> calculated using thermodynamic methods for fluids are greater than the density of water at any temperature; however experimental data show that conditions in which the density of water is greater than that of SO<sub>2</sub> are possible

Naturally, not all the water in the atmosphere would have been under super-critical conditions, but rather only the portion under a pressure higher than the critical pressure of water. Since H<sub>2</sub>O, CO<sub>2</sub> and SO<sub>2</sub> were by far the main

components of the early Earth's atmosphere, analysis of their densities has been conducted for different temperatures and pressures of 10, 25, and 35 MPa (Figs. 2.14, 2.15, 2.16). Data from (Clark 1966; Kerimov et al. 1980; Lide 2005; Speight 2005) were used to calculate the density of H<sub>2</sub>O and CO<sub>2</sub>, and experimental data reported in (Ihmels et al. 2003) for SO<sub>2</sub>. Thermodynamic calculation methods were used to derive the density of SO<sub>2</sub> (Pilchin 2011). This analysis is important for modeling both the conditions at different levels within the atmosphere, and conditions during processes of surface cooling and decline of atmospheric pressures.

The results shown in Fig. 2.16 indicate that the density of water reaches a value of about 75.8 % of the normal density of water (NDW) at 573 K, and decreases drastically to 14.4 % of the NDW at 773 K. Along with the further increase of temperature, the density of water begins to drop much more slowly to a value of about 6 % of the NDW at 1,273 K. Figures 2.14, 2.15 and 2.16 highlight that under specific *P-T*-conditions, the density of water becomes greater than that of SO<sub>2</sub> and CO<sub>2</sub> (see Table 2.23).

Problems related to the evolution of the early Earth's atmosphere during the cooling of the Earth and the formation of the water ocean are discussed in Sect. 6.2.

## References

- Abe Y (1993) Physical state of the very early Earth. *Lithos* 30(3–4):223–235
- Abe Y (1997) Thermal and chemical evolution of the terrestrial magma ocean. *Phys Earth Planet Inter* 100(1–4):27–39
- Adylov GT, Mansurova EP (1999) The use of basalt rocks from koitashskoe ore deposit in production of building ceramics and filter materials. *Glass Ceram* 56(1–2):20–21
- Aleinikov AL, Belikov VT, Eppelbaum LV, Nemzorov NI (2000) Mountainous rock destruction and metamorphic processes in the Earth: a view from classical physics. *Sci Isr* (3):65–87
- Aliev SA, Mekhtiev SF (1970) Geothermics of depression zones of Azerbaijan. Report for 1964–1970. AzTGF, Baku (in Russian)
- Aliev SA, Rustamov RI, Mirzababayev II, Alieva ZA (1977) Geothermal cross-section of forerunner of superdeep Saatly borehole. *Izv AN Azerb SSR, Ser: Earth Sci* 6:115–117 (in Russian)
- Anderson DL (2007) *New theory of the Earth*. Cambridge University Press, Cambridge
- Anderson DL, Whitcomb JH (1973) The dilatancy-diffusion model of earthquake prediction. In: Kovach RL, Nur A (eds) *Proceedings of the Conference on tectonic problems of the San Andreas fault, geological sciences*, vol 13, pp 417–426
- Aronson JR, Bellotti LH, Eckroad SW, Emslie AG, McConnell RK, von Thüna PC (1970) Infrared spectra and radiative thermal conductivity of minerals at high temperatures. *J Geophys Res* 75(17):3443–3456
- Attrill PG, Gibb FGF (2003) Partial melting and recrystallization of granite and their application to deep disposal of radioactive waste: Part 1—rationale and partial melting. *Lithos* 67(1–2):103–117
- Bayly B (1968) *Introduction to petrology*. Prentice-Hall Inc, Englewood Cliffs, NJ

- Best MG (2002) *Igneous and metamorphic petrology*, 2nd edn. Wiley-Blackwell, Hoboken
- Birch F, Clark H (1940) The thermal conductivity of rocks and its dependence upon temperature and composition. *Am J Sci* 238(8):529–558, 613–635
- Birch F, Schairer JF, Spicer HC (eds) (1942) *Handbook of physical constants*. Geological Society of America. Special papers, No. 36
- Blackwell DD, Steele JL (1989) Thermal conductivity of sedimentary rocks: measurement and significance. In: Naeser ND, McCulloch TH (eds) *Thermal history of sedimentary basins*. Springer, New York, pp 5–96
- Blesh CJ, Kulacki FA, Christensen RN (1983) Application of integral methods to prediction of heat transfer from a nuclear waste repository. Open file report ONWI-495, Battelle Memorial Institute, Columbus, OH, 12–17
- Brigaud F (1989) Conductivité thermique et champ de température dans les bassins sédimentaires à partir des données de puits (Documents et Travaux, Centre Géologique et Géophysique de Montpellier)
- Cannat M, Karson JA, Miller DJ et al. (1995) *Proceedings of the ocean drilling program, initial reports*, vol 153
- Čermak V, Rybach L (1982) Thermal conductivity and specific heat of minerals and rocks. In: Angenheister G (ed) *Landolt-Bornstein numerical data and functional relationships in science and technology*. Springer, New York, pp 213–256
- Charles JA (1991) Laboratory shear strength tests and the stability of rockfill slopes. In: Maranhã das Neves E (ed) *Advances in rockfill structures*. Springer, New York, pp 53–72
- CRC Handbook on Chemistry and Physics, 1974. 55th Ed., CRC Press, Florida
- Cheremsky GA (1977) *Applied geothermics*. Nedra, Leningrad (in Russian)
- Cherry JTh, Schock RN, Sweet J (1975) A theoretical model of the dilatant behavior of a brittle rock. *Pure Appl Geophys* 113(1):183–196
- Cho WJ, Kwon S, Choi JW (2009) The thermal conductivity for granite with various water contents. *Eng Geol* 107(3–4):167–171
- Chu J, Kim SR, Oh YN, Balasubramaniam AS, Bergado DT (2004) An experimental and theoretical study on the dilatancy of sand and clays. In: *Proceedings of the 9th Australia–New Zealand Conference on geomechanics*, vol 2, Auckland, New Zealand, pp 654–660
- Clark SP Jr (Ed.) (1966) *Handbook of physical constants* (revised edition). Geological Society of America. Memoir 97, Washington, DC
- Clauser C (1988) Opacity: the concept of radiative thermal conductivity. In: Hänel R, Rybach L, Stegena L (eds) *Handbook of terrestrial heat flow density determination*. Kluwer Academic Publication, Dordrecht, pp 143–165
- Clauser C (2006) Geothermal energy. In: Heinloth K (ed) *Landolt-Börnstein, group VIII: advanced materials and technologies*, vol 3. Energy technologies, Subvol. C: renewable energies, Springer, Berlin, pp 493–604
- Clauser Ch (2009) Heat transport processes in the Earth's crust. *Surv Geophys* 30:163–191
- Clauser C, Huenges E (1995) Thermal conductivity of rocks and minerals. In: Ahrens TJ (ed) *Rock physics and phase relations: a handbook of physical constants*. American Geophysical Union, Reference shelf 3, pp 105–126
- Côté J, Konrad J-M (2005) Thermal conductivity of base-course materials. *Can Geotech J* 42:61–78
- Dakhnov VN (1972) Interpretation of geophysical investigations of borehole sections. Nedra, Moscow (in Russian)
- Dakhnov VN, Dyakonov DI (1952) Thermal investigation of boreholes. Gostoptekhizdat, Leningrad (in Russian)
- Dasgupta R, Hirschmann MM (2007) Effect of variable carbonate concentration on the solidus of mantle peridotite. *Am Mineral* 92:370–379

- Del Gaudio P, Di Toro G, Han R, Hirose T, Nielsen S, Shimamoto T, Cavallo A (2009) Frictional melting of peridotite and seismic slip. *J Geophys Res* 114:B06306. doi:[10.1029/2008JB005990](https://doi.org/10.1029/2008JB005990)
- Dmitriev AP, Kuzyaev LS, Protasov YuI, Yamschikov VS (1969) Physical properties of rocks at high temperatures. Nedra, Moscow (in Russian)
- Dortman NB (ed) (1976) Physical properties of rocks and minerals (petrophysics): handbook of geophysicist. Nedra, Moscow (in Russian)
- Drake MJ (2000) Accretion and primary differentiation of the Earth: a personal journey. *Geochim Cosmochim Acta* 64:2363–2370
- Drake MJ (2005) Origin of water in the terrestrial planets. *Meteoritics Planet Sci* 40:519–527
- Driatskaya ZV, Mkhchiyan MA, Zhmikhova NM (eds) (1971) Oils of the USSR, handbook, vol I, oils of northern regions of the European part of the USSR and the Urals. Khimiya, Moscow (in Russian)
- Driatskaya ZV, Mkhchiyan MA, Zhmikhova NM (eds) (1972) Oils of the USSR, handbook, vol II, oils of the middle and lower Volga region. Khimia, Moscow (in Russian)
- Durham WB, Mirkovich VV, Heard HC (1987) Thermal diffusivity of igneous rocks at elevated pressure and temperature. *J Geophys Res* 92(B11):11615–11634. doi:[10.1029/JB092iB11p11615](https://doi.org/10.1029/JB092iB11p11615)
- ETB (2011) The engineering toolbox. Solids: specific heat capacities
- Eucken A (1911) Dependence of the thermal conductivity of certain gases on the temperature. *Physikal Zeitsch* 12:1101–1107
- Falloon TJ, Green DH, Danyushevsky LV (2007) Crystallization temperatures of tholeiite parental liquids: implications for the existence of thermally driven mantle plumes. In: Foulger GR, Jurdy DM, (eds) Plates, plumes, and planetary processes. The Geological Society of America, special paper 430, Boulder, Colorado, pp 235–260
- Faure G (2000) Origin of igneous rocks: the isotopic evidence. Springer, Berlin
- Faure G, Mensing TM (2007) Introduction to planetary science: the geological perspective. Springer, Berlin
- Genda H, Ikoma M (2008) Origin of the ocean on the Earth: early evolution of water D/H in a hydrogen-rich atmosphere. *Icarus* 194:42–52
- Gillis K, Mével C, Allan J et al (1993) Proceedings of ODP, initial reports, 147: College Station, TX (Ocean Drilling Program). Leg 147
- Golden DC, Ming DW, Lauer HV Jr, Morris RV (2004) Thermal decomposition of siderite-pyrite assemblages: implications for sulfide mineralogy in martian meteorite ALH84001 carbonate globules. *Lunar Planet Sci XXXV*, No. 1396
- Gretener PE (1981) Geothermics: using temperature in hydrocarbon exploration. AAPG, Short Course Notes, 17
- Grove TL, Parman SW (2004) Thermal evolution of the Earth as recorded by komatiites. *Earth Planet Sci Lett* 219:173–187
- Grove TL, Chatterjee N, Parman SW, Medard E (2006) The influence of H<sub>2</sub>O on mantle wedge melting. *Earth Plan Sci Lett* 249:74–89
- Hall H (1995) Igneous petrology. Longman Science and Technology, Singapore
- Hanley EJ, Dewitt DP, Roy RF (1978) The thermal diffusivity of eight well-characterized rocks for the temperature range 300–1,000 K. *Eng Geol* 12:31–47
- Hewins RH, Jones RH, Scott ERD (eds) (1996) Chondrules and the protoplanetary disk. Cambridge University Press, Cambridge
- Hofmeister AM (2007) Pressure dependence of thermal transport properties. *Proc Nat Acad Sci USA* 104(22):9192–9197
- Hofmeister AM, Pertermann M (2008) Thermal diffusivity of clinopyroxenes at elevated temperature. *Eur J Mineral* 20:537–549
- Holland HD (1984) The chemical evolution of atmosphere and oceans. Princeton University Press, Princeton, USA
- Hurtig E, Brugger H (1970) Heat conductivity measurements under uniaxial pressure. *Tectonophysics* 10:67–77

- Ihmels E, Clemmon EW, Gmehling J (2003) An equation of state and compressed liquid supercritical densities for sulfur dioxide. *Fluid Phase Equilib* 207:111–130
- Kappelmeyer O, Hänel R (1974) *Geothermics with special reference to application*. Gebrüder Borntrager, Berlin, Stuttgart
- Kasting JF, Ackerman TP (1986) Climate consequences of very high carbon dioxide levels in the Earth's early atmosphere. *Science* 234:1383–1385
- Kelemen PB, Kikawa E, Miller DJ et al. (2004) *Proceedings of the ocean drilling program, initial reports*, vol 209
- Kerimov KM, Pilchin AN (1986a) Use of geothermics data for prognosis of abnormal stratum pressure and oil and gas perspectives at great depths. In: Kerimov KM (ed) *Combined interpretation of geological-geophysical data with the goal to search oil and gas presence at great depths*. Baku Book Publishers, Baku, pp 25–36 (in Russian)
- Kerimov KM, Pilchin AN (1986b) Geothermal regime of the sedimentary cover of Azerbaijan and Caspian sea depression areas. *Azerbaijan Oil Ind* 1:9–13 (in Russian)
- Kerimov KM, Pilchin AN, Ibragimov SM (1980) Influence of thermodynamical factor on the overhigh pressure in sedimentary strata. *Azerbaijan Oil Industry (Azerbaijanskoe Neftyanoe Khozyaistvo)* 2:6–9 (in Russian)
- Kim J, Lee Y, Koo M (2007) Thermal properties of granite from Korea. *AGU Fall Meeting 2007*, abstract #T11B-0576
- Kukkonen IT, Jokinen J, Seipold U (1999) Temperature and pressure dependencies of thermal transport properties of rocks: implications for uncertainties in thermal lithosphere models and new laboratory measurements of high-grade rocks in the Central Fennoscandian Shield. *Surv Geophys* 20(1):33–59
- Kushiro I, Syono Y, Akimoto S (1968) Melting of a peridotite nodule at high pressures and high water pressures. *J Geophys Res* 73(18):6023–6029
- Kutas RI, Gordienko VV (1971) Heat flow of the Ukraine. *Naukova Dumka, Kiev* (in Russian)
- Labrosse S, Hernlund JW, Coltice N (2007) A crystallizing dense magma ocean at the base of the Earth's mantle. *Nature* 450:866–869
- Lee CTA, Luffi P, Plank T, Dalton H, Leeman WP (2009) Constraints on the depths and temperatures of basaltic magma generation on Earth and other terrestrial planets using new thermobarometers for mafic magmas. *Earth Plan Sci Lett* 279:20–33
- Li J, Agee CB (1996) Geochemistry of mantle-core differentiation at high pressure. *Nature* 381:686–689
- Lide DR (ed) (2005) *CRC handbook of chemistry and physics*, 86th edn
- Litovsky E, Shapiro M (1992) Gas pressure and temperature dependencies of thermal conductivity of porous ceramic materials: part 1, refractories and ceramics with porosity below 30 %. *J Am Ceramic Soc* 75(12):3425–3439
- Liu L (2004) The inception of the oceans and CO<sub>2</sub>-atmosphere in the early history of the Earth. *Earth Planet Sci Lett* 227:179–184
- Lubimova EA (1968a) *Thermics of the Earth and Moon*. Nauka, Moscow (in Russian)
- Lubimova EA (1968a) Thermal history of the Earth. In: *The Earth's crust and upper mantle*. American Geophysical Union, geophysical monograph series, vol 13, pp 63–77
- Lubimova EA, Smirnova EV (1974) Heat physical properties of rocks at high temperatures. In: *Physical properties of rocks under high pressure and temperature*. Trans. of IV All-Union Congress, Tbilisi, pp 171–172 (in Russian)
- Lubimova EA, Lusova LN, Firsov FV (1964) Basics of heat flow from Earth's depths determination and results of measurements. In: *Geothermal researches*. Nauka, Moscow, pp 5–103 (in Russian)
- Lubimova EA, Maslennikov AI, Ganiyev YA (1978) Heat conductivity of sedimentary rocks under elevated pressure and temperatures and polymorphism. In: *Physical properties of rocks under high thermodynamic parameters*. Trans. of IV All-Union Congress, Baku, "Elm" Publication, pp 230–231 (in Russian)

- Magara K (1978) *Compaction and fluid migration: practical petroleum geology*. Elsevier, NY
- Magnitsky VA (1965) *Internal structure and physics of the Earth*. Nedra, Moscow (in Russian)
- Matsui T, Abe Y (1986) Formation of a 'magma ocean' on the terrestrial planets due to the blanketing effect of an impact-induced atmosphere. *Earth Moon Planet* 34:223–230
- McCall GJ (1973) *Meteorites and their origins*. Wiley, NY
- McSween HY Jr (1993) *Stardust to planets*. St. Martin's Griffin, NY
- Mekhtiev SF, Mirzajanzadeh AKh, Aliyev SA (1971) *Geothermal investigation of oil and gas fields*. Nedra, Moscow (in Russian)
- Mekhtiev SF, Kashkay MA, Aliev SA (1972) Investigation of relationships of heat flow with construction and evolution tectonic structure and geophysical fields in different tectonic structures of USSR. (Pre-Kura oil and gas province, Apsheron oil and gas province). Scientific report for 1971–1972. Baku, Azerbaijan Geol. Fund
- Mekhtiev SF, Geodekyan AA, Tsaturyants AB, Ter-Karapetyants ZN, Bayramov EM, Shabanov CF (1973) *Geothermics of oil and gas fields of Azerbaijan and Turkmenistan*. Nauka, Moscow (in Russian)
- Mekhtiev SF, Kerimov KM, Pilchin AN (1982) Role of thermal factors on formation and preservation of AVPD in sedimentary cover of Kura depression. *Azerbaijan Oil Industry (Azerbaijanskoye Neftyanoye Khozyaystvo)* 3:1–5 (in Russian)
- Mekhtiev SF, Kerimov KM, Pilchin AN, Agabekov AM (1985) Geothermal regime of depression zones of the Caucasus and SW part of Turanskaya plate and its influence on formation of abnormal pressures within their deposits. In: Ismail-Zade TA et al. (eds) *Trans. of Scien-Tech. Meet. Geological-geophysical methods of searching oil and gas fields at great depths*, Baku, pp 76–78 (in Russian)
- Morse JW, Mackenzie FT (1998) Hadean ocean carbonate geochemistry. *Aquat Geochem* 4(3–4):301–319
- Nikonova NS, Tikhomirova IN, Belyakov AV, Zakharov AI (2003) Wollastonite in silicate matrices. *Glass Ceram* 60(9–10):342–346
- Nur A (1972) Dilatancy, pore fluids, and premonitory variations of  $T_S/T_P$  travel times. *Bull Seismol Soc Am* 62(5):1217–1222
- Nur A (1975) A note on the constitutive law for dilatancy. *Pure Appl Geophys* 113(1):197–206
- Pender MJ (1978) A model for the behaviour of overconsolidated soils. *Geotechnique* 28(1):1–25
- Pertermann M, Hofmeister AM (2006) Thermal diffusivity of olivine-group minerals at high temperature. *Am Mineral* 91(11–12):1747–1760
- Petrinin GI, Popov VG (1995) Temperature dependence of lattice thermal conductivity of Earth's mineral substance. *Izv Russ Acad Sci, Phys Solid Earth* 30(7–8)
- Pilchin AN (1978a) Correction to hydrostatic pressure in the crust of the Middle Kura depression. In: *Geophysical researches of the oil, gas and ore deposits in Azerbaijan*, Baku, pp 78–80 (in Russian)
- Pilchin A (1983) *Geothermal regime of Earth's crust of the Kura depression and its influence on pressure distribution in it*. Ph.D. thesis, Institute of Geophysics of the Georg. Academy of Science, Tbilisi (in Russian)
- Pilchin AN (2011) Magnetite: the story of the mineral's formation and stability. In: Angrove DM (ed) *Magnetite: structure, properties and applications*. Nova Science Publishers, NY, pp 1–99 Chapter 1
- Pilchin AN, Eppelbaum LV (2002) Some peculiarities of thermodynamic conditions of the Earth crust and upper mantle. *Sci Isr* 4(1–2):117–142
- Pilchin AN, Eppelbaum LV (2004) On the stability of ferrous and ferric iron oxides and its role in rocks and rock-forming minerals stability. *Sci Isr* 6(3–4):119–135
- Pilchin AN, Eppelbaum LV (2006) *Iron and its unique role in earth evolution*. Monograph 9, Mexican Geophysics Soc



- Pilchin AN, Eppelbaum LV (2009) The early Earth and formation of the lithosphere. In: Anderson JE, Coates RW (eds) *The Lithosphere: Geochemistry, Geology and Geophysics*. Nova Science Publishers, NY, pp 1–68 Chapter 1
- Pilchin AN, Kerimov KM (1986) Some features of abnormality of pressure coefficient change in collectors with different character of saturation. In: Mikhailov IM, Rizhik VM, Shendrey LP (eds) *Role of abnormal pressures in oil and gas field distribution*. IGIRGI Publishers, Moscow, pp 140–143 (in Russian)
- Poelchau HS, Baker DR, Hantschel Th, Horsfield B, Wygrala B (1997) Basin simulation and the design of the conceptual basin model. In: Welte DH, Horsfield B, Baker DR (eds) *Petroleum and basin evaluation*. Springer, Berlin, pp 36–41
- Pollack HN (1997) Thermal characteristics of the Archaean. In: de Wit MJ, Ashwal MD (eds) *Greenstone belts*. Clarendon Press, Oxford, UK, pp 223–232
- Popov YA, Pevzner LA, Romushkevich RA, Korostelev VM, Vorob'yev MG (1995) Thermophysical and geothermal sections obtained from Kolvinskaya well logging data. *Izv Acad Sci Russ, Phys Solid Earth* 30:778–789
- Popov Y, Tertychnyi V, Romushkevich R, Korobkov D, Pohl J (2003) Interrelations between thermal conductivity and other physical properties of rocks: experimental data. *Pure Appl Geophys* 160:1137–1161
- Prats M (1982) *Thermal recovery*, vol 7., Monograph Series Society of Petroleum Engineers, Dallas
- Pribnow D, Williams CF, Sass JH, Keating R (1996) Thermal conductivity of water-saturated rocks from the KTB pilot hole at temperatures of 25 to 300 °C. *Geophys Res Lett* 23(4):391–394
- Proselkov YM (1975) Heat transfer in wells. Nedra, Moscow (in Russian)
- Rau H, Kuttly TRN, Guedes de Carvalho JRF (1973) High temperature saturated vapor pressure of sulphur and the estimation of its critical quantities. *J Chem Thermodyn* 5:291–302
- Ray L, Roy S, Srinivasan R (2008) High radiogenic heat production in the Kerala Khondalite block, Southern Granulite province, India. *Int J Earth Sci* 97(2):257–267
- Reid RC, Prausnitz JM, Poling BE (1987) *The properties of gases and liquids*, 4th edn. McGraw-Hill, NY
- Reynolds O (1885) On the dilatancy of media composed of rigid particles in contact. *Philos Mag* 5(20):469–482
- Righter K, Drake MJ (1997) Metal-silicate equilibrium in a homogeneously accreting earth: new results for Re. *Earth Planet Sci Lett* 146(3–4):541–553
- Robertson EC (1979) *Thermal conductivity of rocks*. U.S. Geological Survey open file report 79–356
- Roscoe KH, Burland JB (1968) On the generalized stress–strain behaviour of wet clay. In: *Engineering plasticity*, Cambridge, pp 535–609
- Roscoe KH, Schofield AN, Thurairajah A (1963) Yielding of clays in state Wetter than critical. *Geotechnique* 13(3):211–240
- Rowe PW (1962) The stress-dilatancy relation for static equilibrium of an assembly of particles in contact. *Proc R Soc London, Ser A* 269:500–527
- Sass JH, Lachenbruch AH, Munroe RJ, Greene GW, Moses TH Jr (1971) Heat flow in the western United States. *J Geophys Res* 76:6376–6413
- Schärli U, Rybach L (2001) Determination of specific heat capacity on rock fragments. *Geothermics* 30:93–110
- Schofield AN, Wroth CP (1968) *Critical state soil mechanics*. McGraw-Hill, London
- Scholz CH, Sykes LR, Aggarwal YP (1973) Earthquake prediction: a physical basis. *Science* 181(4102):803–810
- Schubert G, Turcotte DL, Olson P (2001) *Mantle convection in the Earth and Planets two volume set*. Cambridge University Press, Cambridge
- Seipold U (2002) Investigation of the thermal transport properties of amphibolites: I. pressure dependence. *High Temp High Pressures* 34(3):299–306

- Seipold U, Gutzzeit W (1980) Measurements of the thermal properties of rocks under extreme conditions. *Phys Earth Planet Inter* 22(3–4):267–271
- Seipold U, Huenges E (1998) Thermal properties of gneisses and amphibolites: high pressure and high temperature investigations of KTB-rock samples. *Tectonophysics* 291(1–4):173–178
- Sharma PV (2002) *Environmental and engineering geophysics*. Cambridge University Press, Cambridge
- Shim BO, Park JM, Kim HC, Lee Y (2010) Statistical analysis on the thermal conductivity of rocks in the Republic of Korea. In: *Proceedings of the World Geothermal Congress 2010*, Bali, Indonesia
- Sibson RH (1981) Controls on low-stress hydro-fracture dilatancy in thrust, wrench and normal fault terrains. *Nature* 289:665–667
- Simmons G (1961) Anisotropic thermal conductivity. *J Geophys Res* 66(7):2269–2270
- Sleep NH, Zahnle K, Neuhoﬀ PS (2001) Initiation of clement surface conditions on the earliest Earth. *Proc Natl Acad Sci US* 98(7):3666–3672
- Solomatov VS (2000) Fluid dynamics of a terrestrial magma ocean. In: Canup R, Righter K (eds) *Origin of the Earth and Moon*. University of Arizona Press, Tucson, Arizona, pp 323–338
- Somerton WH (1958) Some thermal characteristics of porous rocks. *Trans AIME* 213:375–378
- Somerton WH (1992) Thermal properties and temperature related behavior of rock/fluid systems. *Developments in Petroleum Science*, 37. Elsevier, Amsterdam
- Speight JG (2005) *Lange's handbook of chemistry*, 16th edn. McGraw-Hill, NY
- Spohn T, Schubert G (1991) Thermal equilibration of the Earth following a giant impact. *Geophys J Int* 107:163–170
- Starikova GN, Lubimova EA (1973) Heat properties of rocks from Kola peninsula. In: *Heat flows from Earth crust and upper mantle*. Nauka, Moscow, pp 112–124 (in Russian)
- Stimpfl M, Lauretta DS, Drake MJ (2004) Adsorption as a mechanism to deliver water to the Earth (abstract). *Meteorit Planet Sci* 39:A99
- Stoiber RE (1995) Volcanic gases from subaerial volcanoes on Earth. In: *Global earth physics, a handbook of physical constants*. AGU, Ref. Shelf 1, pp 308–319
- Sukumaran PV (2001) Early planetary environments and the origin of life. *Resonance* 6(10):16–28
- Tamura Y, Yuhara M, Ishii T, Irino N, Shukuno H (2003) Andesites and dacites from Daisen volcano, Japan: partial-to-total remelting of an andesite magma body. *J Petrol* 44(12):2243–2260
- Téqui C, Robie RA, Hemingway BS, Neuville DR, Richet P (1991) Melting and thermodynamic properties of pyrope ( $\text{Mg}_3\text{Al}_2\text{Si}_3\text{O}_{12}$ ). *Geochim Cosmochim Acta* 55(4):1005–1010
- Textor C, Graf H-F, Timmreck C, Robock A (2004) Emissions from volcanoes. In: Granier C, Reeves C, Artaxo P (eds) *Emissions of chemical compounds and aerosols in the atmosphere*. Kluwer, Dordrecht, pp 269–303 Chapter 7
- Thy P, Leshner CE, Mayfield JD (1999) Low-pressure melting studies of basalt and basaltic andesite from the southeast Greenland continental margin and the origin of dacites at site 917. In: Larsen HC, Duncan RA, Allan JF, Brooks K (eds) *Proceedings of the ocean drilling program, scientific results*, 163, Scient. Res. southeast Greenland Margin, Chapter 9, pp 95–112
- Valley JW, Peck WH, King EM, Wilde SA (2002) A cool early Earth. *Geology* 30(4):351–354
- Van Westrenen W, Wood BJ, Blundy JD (2001) A predictive thermodynamic model of garnet-melt trace element partitioning. *Contrib Mineral Petrol* 142:219–234
- Volarovich MP (ed) (1978) *Handbook on physical properties of minerals and rocks under high thermodynamic parameters*. Nedra, Moscow (in Russian)
- Vosteen H-D, Schellschmidt R (2003) Influence of temperature on thermal conductivity, thermal capacity and thermal diffusivity for different types of rock. *Phys Chem Earth* 28:499–509
- Walker JCG (1985) Carbon dioxide on the early Earth. *Orig Life Evol Biosph* 16(2):117–127

- Walter MJ, Trønnes RG (2004) Early Earth differentiation. *Earth Planet Sci Lett* 225(3–4):253–269
- Wan RG, Guo PJ (2004) Stress dilatancy and fabric dependencies on sand behavior. *J Eng Mech* 130(6):635–645
- Waples DW, Waples JS (2004) A review and evaluation of specific heat capacities of rocks, minerals, and subsurface fluids. Part 1: minerals and nonporous rocks. *Nat Resour Res* 13(2):97–122
- Wenk H-R, Bulakh AG (2004) *Minerals: their constitution and origin*. Cambridge University Press, Cambridge
- Whittington AG, Hofmeister AM, Nabelek PI (2009) Temperature-dependent thermal diffusivity of the Earth's crust and implications for magmatism. *Nature* 458:319–321
- Yaws CL (2001) *Matheson gas data book*, 7th edn. McGraw-Hill, New York
- Yaws CL (2008) *Thermophysical properties of chemicals and hydrocarbons*. William Andrew, Norwich
- Yoder HS Jr (1976) *Generation of basaltic magma*. National Academy of Science, Washington, DC
- Zahnle KJ, Kasting JF, Pollack JB (1988) Evolution of a steam atmosphere during Earth's accretion. *Icarus* 74:62–97
- Zhang Y, Zindler A (1993) Distribution and evolution of carbon and nitrogen in Earth. *Earth Planet Sci Lett* 117:331–345
- Zinger AS, Kotrovsky VV (1979) Hydro-geothermal conditions of water systems of western part of Pre-Caspian depression. Saratov University, Saratov (in Russian)
- Zoth G, Hänel R (1988) Appendix. In: Hänel R, Rybach L, Stegena L (eds) *Handbook of terrestrial heat flow density determination*. Kluwer, Dordrecht, pp 449–466

Applied Geothermics

Eppelbaum, L.; Kutasov, I.; Pilchin, A.

2014, XVIII, 751 p. 204 illus., 21 illus. in color.,

Hardcover

ISBN: 978-3-642-34022-2